

Improved Prediction Of Ligand-Protein Binding Affinities By Meta-Modeling

Ho-Joon Lee^{1,2,*#}, Prashant S. Emani^{3,*#} and Mark B. Gerstein^{3,4,5,6,7#}

¹Dept. of Genetics and ²Yale Center for Genome Analysis, Yale University, New Haven, CT 06510, USA

³Dept. of Molecular Biophysics & Biochemistry, Yale University, New Haven, CT 06520, USA ⁴Program in Computational Biology & Bioinformatics, ⁵Dept. of Computer Science, ⁶Dept. of Statistics & Data Science, and ⁷Dept. of Biomedical Informatics & Data Science, Yale University, New Haven, CT 06520, USA

* Equal contributions

Correspondence: HL, ho-joon.lee@yale.edu; PSE, prashant.emani@yale.edu; MBG, pi@gersteinlab.org

Abstract

The accurate screening of candidate drug ligands against target proteins through computational approaches is of prime interest to drug development efforts. Such virtual screening depends in part on methods to predict the binding affinity between ligands and proteins. Many computational models for binding affinity prediction have been developed, but with varying results across targets. Given that ensembling or meta-modeling methods have shown great promise in reducing model-specific biases, we develop a framework to integrate published force-field-based empirical docking and sequence-based deep learning models. In building this framework, we evaluate many combinations of individual base models, training databases, and several meta-modeling approaches. We show that many of our meta-models significantly improve affinity predictions over base models. Our best meta-models achieve comparable performance to state-of-the-art deep learning tools exclusively based on structures, while allowing for improved database scalability and flexibility through the explicit inclusion of features such as physicochemical properties or molecular descriptors. Overall, we demonstrate that diverse modeling approaches can be ensembled together to gain improvement in binding affinity prediction.

Introduction

Molecular interactions such as protein-protein or ligand-protein interactions are fundamental processes in biology as well as biophysics and biochemistry. Knowledge of interaction energy or binding affinity is essential in understanding biological functions and biomedical applications. In drug discovery or development, accurate prediction of binding affinity of a drug ligand bound to a target molecule (typically a protein) is of central importance in identifying the most stable structure of a drug-target complex, i.e., the best 3-dimensional pose (geometry) of a drug in the binding pocket of a target molecule, known as molecular docking. Along with development of molecular docking algorithms, there have been extensive computational studies with decades of efforts to achieve better prediction of ligand-protein binding affinity with applications to high throughput drug screening or virtual screening¹⁻¹⁰. This has been achieved by various scoring functions that represent the binding free energy or stability of a ligand-protein complex and select the best docking pose. Docking tools typically generate multiple candidate poses of a ligand and rank them by binding affinity scores. Therefore, accurate prediction of binding affinity is critical in drug discovery and development. Scoring functions were developed traditionally by *ab initio* physical force field-based, knowledge-based, or empirical methods, or more recently by advanced machine learning or deep learning approaches.

The predictive power of traditional or classical scoring functions is known to be very limited due to rigid or naive underlying assumptions^{1, 5}, e.g. reliance on linear regression^{11, 12} or over-simplification or ignorance of desolvation and entropy contributions because of computational cost¹³⁻¹⁵. In addition, previous evaluation studies of more than a dozen scoring functions reported that no scoring function was consistently better than others in all conducted tests, showing both strengths and weaknesses for different purposes¹⁶⁻¹⁸. For example, the best scoring function in terms of a prediction correlation with experimental binding affinities was not necessarily best in terms of predicting correct ligand poses (i.e., not the lowest prediction errors). Despite those limitations, classical scoring functions (especially empirical ones) have been widely used and implemented in several software tools such as Autodock Vina¹⁹ or *smina*²⁰. Furthermore, consensus scoring strategies from multiple scoring functions have shown improved performances^{16, 21-24}.

In continued efforts to improve prediction accuracy, advanced machine or statistical learning-based regression methods such as Random Forests, support vector machines, or neural networks have been successfully used to develop alternative scoring functions by leveraging large-scale databases such as PDBbind²⁵ for more diverse physicochemical and geometric features of ligand-protein complexes and their experimental binding affinities^{1, 3, 11, 26-28}. Improved performance of machine learning (ML) methods is mainly due to their ability to leverage big data and engineered features to capture non-linear or non-additive relationships in binding or docking that are likely to be missed by classical scoring functions²⁹. Furthermore, with the groundbreaking advancement of deep learning (DL) in computer science, its applications in biomedicine, including protein structure prediction, binding affinity prediction, and drug discovery, have been very successful and promising^{1, 27, 30-39}. Deep learning methods for binding affinity prediction are advanced regression methods that typically generate sophisticated abstract representations or embeddings for ligands, proteins, or ligand-protein complexes via various neural network architectures to learn hidden patterns. Inspired by the breakthroughs in computer vision^{40, 41}, various DL models based on convolutional neural networks (CNNs) have been developed using 3-dimensional (3D) structural information of ligand-protein complexes with high prediction accuracies superior to those advanced ML models mentioned above⁴²⁻⁵⁰. In addition, methods based on graph neural networks have been successful as well^{42, 47, 51-56}. On the other hand, DL methods with ligand and protein sequences alone, i.e., without structural information, have also shown comparable performances^{57, 58}. In general, DL architectures are highly diverse with a number of hyperparameters such as the network depth and width, loss and activation functions, and a learning rate, which makes model optimization very challenging due to high computational

cost. More importantly, fundamental issues with DL approaches have been interpretability or explainability of their non-intuitive excellent performances⁵⁹⁻⁶³. On another note, mathematically advanced methods such as differential geometry and/or algebraic topology-based analyses in combination with ML or DL regression have been also developed showing notably improved performances in ligand-protein binding affinity prediction⁶⁴⁻⁷¹, as well as physics-based hybrid models^{72, 73}.

In this work, we aim to improve ligand-protein binding affinity prediction by combining both classical scoring functions, which are built upon physical force fields, and sequence-based DL models into a single integrative framework of meta-models (also called ensemble, fusion, or hybrid models). Meta-models are a type of ensemble learning by combining diverse algorithms and have been successful in machine or statistical learning for improved results with more robustness and less bias than individual algorithms (known as stacked generalization or super learning)^{74, 75}. Meta-models, termed *blending* in associated publications, were also very successful in addressing the Netflix Prize challenges⁷⁶⁻⁷⁹. In predicting ligand-protein binding affinity, ensemble models of multiple 3D CNNs have been shown to outperform single CNNs and previous models⁵⁰. On the other hand, theory-driven physical models and data-driven ML or statistical models are complementary to each other. The former offers physical interpretability and constraints, whereas the latter is better at complex pattern discovery from massive data. For this reason, hybrid approaches have been favored in recent years^{72, 73, 80-83}. In general, the intuition behind meta-modeling is that different solutions to a problem could be modeling non-overlapping aspects of the ground truth. These different solutions may be trained on data with their own systematic biases, or might have architectures that access some limited subspace of the possible model space. When combined, an ensemble of such solutions might serve to better represent the ground truth. We have designed a modeling framework that allows the inclusion of structure-based classical scoring functions and sequence-based DL models, as well as explicit inclusion of covariates such as physicochemical features of ligand, proteins, or ligand-protein complexes (**Figure 1 and Supplementary Figure S1**). In this study, we first focus on 2 empirical scoring functions (ESFs), SMINA and Vinardo (implemented in *smina*)²⁰ together with consensus docking strategies based on experimental or predicted ligand poses. For DL models, we use sequence-based DL models of 10 different architectures with multiple training strategies, employing an open-source DL library for drug-target interaction prediction called DeepPurpose⁵⁷ and two ligand-protein binding databases, BindingDB⁸⁴ and PDBbind. We investigate both pre-trained models from the DeepPurpose library and our own fine-tuned or *de novo*-trained models using PDBbind, which is the main data used by the ESF models. In addition, by merging all prediction scores from repeated cross-validations for all DL models under study, we investigate top principal components from principal component analysis (PCA) as additional prediction scores. Finally, by taking all prediction scores from both ESF and DL models as well as molecular weights of ligands, we build meta-models using 4 machine learning algorithms and 11 feature sets as our final tools (44 in total) for ligand-protein binding affinity prediction.

Using a benchmark dataset of CASF-2016⁷ and a small-scale virtual screening, we demonstrate that our meta-models outperform individual base models and exhibit competitive performance to more sophisticated structure-based DL models, serving as a potentially useful general framework for continual future improvement of ligand-protein binding affinity prediction. The advantages offered by such an approach over existing methods include: (1) scalability by utilizing sequence-based databases for DL models without the need for 3D structures; and (2) flexibility by allowing different base models and physicochemical or molecular properties to be incorporated into meta-models. We believe that such an extensive exploration of these aspects of binding affinity prediction makes a meaningful contribution to the discussion of model generalization.

Methods

Dataset selection

BindingDB

We used the BindingDB ver. 2020m2 database (<http://www.bindingdb.org>) for the purpose of DL model training. A total of 66,444 ligand-protein complexes from the Ligand-Target-Affinity dataset were filtered with $K_d \leq 0.01M$, valid PubChem IDs or InChI keys for ligands, and valid UniProt IDs for proteins.

PDBbind

We downloaded the PDBbind v2020 *refinedset* from <http://www.pdbbind.org.cn/>. The dataset consisted of 5,316 target protein-drug ligand complexes. The *refined set* (labeled RefinedSet) has been filtered by the PDBbind creators from a larger dataset by the removal of complexes that have “obvious problems in 3D structure, binding data or other aspects”⁸⁵. Of these, 285 ligand-protein complexes are in the so-called *coreset* (labeled CoreSet), which are high-quality data that are used as the primary test set for the Comparative Assessment of Scoring Functions (CASF) benchmark⁷. This CoreSet was separated from the remainder of the PDBbind RefinedSet to serve as an external test set (i.e., benchmark set) for evaluating model performance. Thus, we consider a training set of 5,031 ligand-protein complexes and an external test set of 285 complexes. Binding affinity values we used in this study were the natural logarithms of K_d or K_i values. We did not distinguish K_d and K_i from each other.

Molecular docking

Implementation of ligand docking

We employ the *smi* implementation²⁰ of the AutoDock Vina method¹⁹ for the docking component. The *smi* implementation is designed to make AutoDock easier to use, with larger support for ligand molecular formats and improved minimization algorithms. We used both the default SMINA scoring function and another previously published scoring function, Vinardo⁸⁶, provided in *smi*. We note that the italicized *smi* describes the program while the capitalized SMINA describes the scoring function. In the meta-models below, we refer to this class of empirical docking methods as E. The tandem use of both scoring functions is meant to address possible idiosyncrasies in the parameterizations of the scoring functions. *smi* is run as a command-line program using a receptor structure in PDBQT format and a ligand in 3D SDF format. Our in-house Python script includes steps for the preparation of the receptor structures, the creation of the configuration file, and the running of *smi* (**Supporting Information**). The output for each scoring function consists of the binding affinities for the 9 (the default option) best docking poses. Seven complexes with multiple ligands (whose names were separated with “&” or “/”) in the PDBbind dataset were not docked as there was some ambiguity as to which ligand to consider in the docking. These complexes were excluded from further analyses.

Processing of docking scores

Previous studies have demonstrated the value of (a) filtering the docking poses output by empirical docking programs based on the degree to which they agree with experimental scores²⁰ and (b) comparing poses from two or more docking methods, in so-called “consensus” approaches, and filtering based on the degree of agreement to yield a higher quality output^{23, 24, 87}. Accordingly, we carried out preprocessing of the docking scores by filtering out certain complexes based on the quality of the associated poses assessed by these two criteria. For each complex out of the available 9 docking poses, we calculated the root-mean-square deviation (RMSD) between docking poses in two different ways (described below), and utilized the RMSD value as a cutoff in determining the best set of binding affinities to choose in the final dataset to the meta-models. The goal was to determine if pose quality, either relative to an available

experimental gold-standard or relative to the results of another scoring function, would impact both the matching of the predicted binding affinity as well as the downstream prediction process.

We choose to implement the symmetric RMSD employed by Trott and Olson¹⁹ using Pymol’s Python API. In brief, this RMSD is calculated between two different ligand structures as $RMSD_{ab} = \max(R_{a\setminus b}, R_{b\setminus a})$ where $R_{a\setminus b}$ describes an asymmetric measure of distance:

$$R_{a\setminus b} = \sqrt{\frac{1}{N} \sum_i \min_j r_{ij}^2}$$

where the summation is over all N heavy atoms in structure a , the minimum is over all atoms (j) in structure b of the same element type as atom i in structure a .

We calculate $RMSD_{ab}$ in two ways, depending on the choice of docking poses: (1) Experimental pose-RMSD filtering, where the RMSD is calculated for a ligand pose predicted by a docking method relative to the experimental structure of the ligand (when available); and (2) Consensus pose-RMSD filtering, where the RMSD is calculated between the docking poses for the same ligand-target pair as predicted by two different docking scoring methods, Vinardo and SMINA. Details of these filtering approaches are provided in **Supporting Information**. We also chose a cutoff of 3 Angstroms as representing a reasonably good quality match between poses based on our manual inspection of RMSD distributions (**Supplementary Figure S2A**). This is a more lenient cutoff relative to other analyses^{20, 23} that suggest a 2-Angstrom cutoff. Our approach is a compromise between the need for higher quality matches, and the need to have sufficient numbers of data points to train our models as stricter cutoffs lead to smaller dataset sizes.

An important aspect of these parallel approaches to applying the RMSD filters on the data is that the scores extracted from the empirical docking runs are different when considering the Experimental RMSD filter and the Consensus RMSD filter. This is even the case when considering the unfiltered dataset, where the set of complexes are identical, but the choice of poses used to extract the best docking scores differ between the two RMSD filter approaches. Finally, we note that, in the naming of the model files, we use the shorthand “VvS” to indicate the Consensus RMSD filtering as the comparison involves Vinardo versus SMINA poses.

Deep Learning

DeepPurpose library

We used the Python library, DeepPurpose, for deep learning of binding affinities of ligand-target complexes⁵⁷. It offers a framework for various models that combine ligand-encoding and protein-encoding neural networks. We modified and customized the version 0.0.1 of the library (as of July 24, 2020) for development of our work, while all 6 pre-trained models with BindingDB-2020m2-Kd were downloaded from the version 0.1.5 (as of June 29, 2022). The 6 pre-trained models are CNN-CNN, Daylight-AAC, Morgan-AAC, Morgan-CNN, MPNN-CNN, and Transformer-CNN. We refer to this class of BindingDB pre-trained models as D1.

Training of 12 DL models from the DeepPurpose library using BindingDB

The DeepPurpose library offers various embedding methods for both ligands and proteins to build regression models to predict binding affinities of ligand-protein complexes. After initial pilot experiments, we chose the following 12 models of ligand-protein embedding methods for downstream analyses: CNN-CNN, Daylight-AAC, Morgan-AAC, Morgan-CNN, MPNN-CNN, Transformer-CNN, MPNN-Quasi-seq, CNN/RNN-CNN/RNN, CNN-AAC, MPNN-Transformer, MPNN-PseudoAAC, MPNN-AAC, MPNN-CNN/RNN, Transformer-Quasi-seq, and Transformer-Transformer. We applied the 12 models to BindingDB Kd data, which were used by the DeepPurpose library. Their 6 pre-trained

models mentioned above were reported to achieve performances of mean 5-fold cross-validated MSE < 0.6 or Pearson correlation coefficient (PCC) < 0.8 ⁵⁷. Given the published results of their best models, we re-trained or *de novo*-trained all 12 models from scratch to either reproduce their best models or identify more models with similar performances for our downstream model development. We used all default hyperparameters for each model in DeepPurpose and did not perform cross validation given the target performance of MSE = 0.6 or PCC = 0.8. The data split for training, validation, and testing was 70% (46,511 cpx), 10% (6,644 cpx), and 20% (13,289 cpx), respectively, with random seed = 1. Those top models selected with the target performance are considered as crude or low-confidence deep learning models, being a starting point in our entire pipeline for the sake of computational efficiency given limited resources. We refer to this class of BindingDB *de novo*-trained models as D2.

Training of DL models using PDBbind

We also trained 10 DL models using the PDBbind RefinedSet binding affinity data (Kd/Ki) that contain ligand-target structural data and were used by the docking tools. The 10 models come from the 6 pre-trained models and the top 6 *de novo*-trained models selected from above (two models in common). This is to compare with the BindingDB-trained DL models. We excluded the CASF2016 CoreSet within the PDBbind RefinedSet, which we use for external validation, and performed 10x repeated 5-fold cross validation with random seed = 1701. We refer to this class of PDBbind-trained models as D3.

Fine-tuning of the BDB-trained models using PDBbind

In order to leverage the respectable performance of the BindingDB-trained models (D1 and D2), we finetuned them using the PDBbind data excluding the CoreSet (referred as D1F and D2F, respectively). To increase analysis robustness, we performed iterative 5-fold CV with 10 iterations, i.e., 50 validations (using the scikit-learn function in Python, RepeatedKFold or KFold, with random_state=1701) for each of the 6 D1F, 6 D2F, and 10 D3 models to yield 300, 300, 500 model variants or predictions, respectively. We also performed PCA on those predictions for the 3 model classes (referred as D1FP, D2FP, D3P, respectively) as well as on the merged 1,100 predictions (referred as DAP) for ML meta-models below for dimensionality reduction of the meta-features (predictors).

Machine Learning Meta-Models

The fact that we have two independent approaches of quantifying the binding affinities (i.e. docking and deep learning tools) means that we potentially have complementary sources of information in the data. The docking tools are based on empirical scoring functions trained to match experimental structural data, while the deep learning tools capture information on the sequences of ligands and proteins. The exact partition of dual sequence/structure impacts on the results from these two approaches is not entirely clear, but the expectation is that there is likely non-overlapping information contained in the predictions of these approaches. Accordingly, we have sought to exploit any complementary information by feeding the docking and deep learning scores into a set of linear and non-linear machine learning models to gain improvements in prediction of binding affinities. We term these machine learning models as *meta-models* since they incorporate predictions from independent tools as base models. We used linear regression, ElasticNet, and LASSO algorithms for linear meta-models and the XGBoost algorithm for a non-linear meta-model implemented in *scikit-learn* in Python. Hyperparameter optimization was done along with multiple 5-fold cross validations. Details are given in **Supporting Information**.

The features for the meta-models are SMINA and Vinardo predictions with different RMSD filtering cutoffs, ligand molecular weights (MWs), and DL predictions. We experimented with various combinations of those features: (1) SMINA + Vinardo (with/without the filters) (2) SMINA + Vinardo (with/without

the filters) + MW (3) SMINA + Vinardo + MW + DL mean predictions (BindingDB or PDBbind) and (4) SMINA + Vinardo + MW + DL PCA projections (BindingDB or PDBbind). For the BindingDB-trained scores, we used the top 6 models as described above. For the DL models fine-tuned on the PDBbind dataset, we take the mean of the 50 CV predictions for each of the 6 models (i.e., 6 meta-model features). For the PCA of all DL scores, we also ran an optimization over the number of principal components (PCs) to include as features. We allowed for between 1 and 22 top principal components to be included (i.e., PC 1, PCs 1-2, PCs 1-3, . . . PCs 1-22), and the selection of the best model among the 22 options was done by maximizing the Pearson correlation for each of the 4 meta-models separately using 20% of the training data as a leave-out validation set for hyperparameter optimization. We chose to optimize up to the top 22 PCs to match the number of models used in all the deep learning runs in D1, D2 and D3 combined.

Each of the optimized meta-models generated above is tested against the CoreSet using the relevant meta-model-specific feature sets. For all meta-models, the Pearson correlation, the Spearman rank correlation, the mean-square error (MSE), and the root-mean-square error (RMSE) for the CoreSet predictions were calculated and reported for model evaluation. A detailed description of these meta-model features is shown in **Table 1**.

SwissADME and UniProt Analysis

To understand the contributions of ligand properties to benchmark performance of all the models, we used the web tool *SwissADME*⁸⁸ to extract the properties of the PDBbind CoreSet ligands from their SMILES strings. Also, we investigated the SwissADME features that might be associated with better or worse performance for subsets of complexes by the different groups of tools (docking, DL, and meta-models). To evaluate the contributions of protein features, we extracted the relevant subsets of PDBbind CoreSet PDB IDs from our analyses and fed them into the “Retrieve/ID mapping” tool of the UniProt database⁸⁹. We studied the resulting protein properties (e.g. pathway information) for over- or under-representation in our predictions. Details are provided in **Supporting Information**.

Virtual Screening Benchmarks

To test the possibility of certain tools performing the prediction task with differing degrees of accuracy for certain proteins or even families of proteins, we devised a virtual screening test by selecting 3 most frequently targeted proteins by multiple ligands from the general set of PDBbind v2020 (GeneralSet) excluding the RefinedSet we used for model training. We considered only those proteins in GeneralSet whose sequence similarity to those in RefinedSet was found to be less than 30% by the NCBI Blastp package⁹⁰. We also filtered out complexes in the GeneralSet that had only IC50 experimental measurements for consistency with this study. The resulting top 3 proteins are O60341, O15151, and P0C6U8 (UniProt Accession IDs), which are complexed with 20, 8, and 7 ligands, respectively. The resolution of the 35 complexes ranges from 1.33 to 3.50 Angstroms with mean of 2.58 and standard deviation of 0.69.

For a more general applicability, we also performed a virtual screening using an external benchmark dataset, LIT-PCBA, of active and inactive ligands for 15 target proteins⁹¹. Although our models were neither explicitly designed nor trained to distinguish active and inactive ligands from each other (i.e., binary classification for functional activity), our assumption was that active ligands tend to have higher binding affinities (i.e., lower Kd/Ki) for target proteins than inactive ligands. This assumption is weak because there is an unclear causal relationship between binding affinity (Kd, Ki) and functional activity (IC50, EC50). We also note that we used ligand-protein complexes with Kd or Ki from both BindingDB and

PDBbind for consistency. LIT-PCBA is a recently developed virtual screening dataset which was reported to be less biased than previous datasets. It is based on PubChem BioAssays which includes 4 potency types of IC50, EC50, Kd, and Ki. We point out that LIT-PCBA did not distinguish the 4 potency types from each other. As a proof-of-concept, with the aforementioned caveat in mind, we randomly selected 10 active and 10 inactive ligands for each of the 15 proteins in LIT-PCBA (i.e., a total of 300 ligand-protein pairs) to predict their binding affinities by our models. The active and inactive ligands were chosen from the combined training and validation sets in LIT-PCBA. We generated three-dimensional SDF files for each of the ligands from the SMILES strings. We also randomly selected only one of the PDB structures (in mol2 format) for each target protein in this virtual screening exercise (further details in **Supporting Information**). The evaluation was done in two ways: (1) comparisons of predicted binding affinity distributions between active and inactive ligands for each protein with Wilcoxon and Mann-Whitney U tests for significant differences; (2) an enrichment or fraction of active ligands in the top 5 highest-affinity ligands predicted for each protein (i.e., in the top 25% of the 20 evaluated ligands for each protein).

Results

Docking tools

We ran *smina* with two different scoring functions, SMINA and Vinardo (model class E), on the PDBbind dataset. We distinguish the PDBbind “RefinedSet” excluding the “CoreSet” (designated as “RefinedSet\CoreSet”) from the “CoreSet” which is used as the external validation (benchmark) set in this study. Additionally, as described in the Methods, we considered two formulations of the docking pose-based RMSD for the 9 poses generated by the docking tools for each protein-ligand complex: an “Experimental” RMSD relative to the experimental pose, and a “Consensus” RMSD. We indicate the unfiltered dataset by RMSD < 101 Angstroms, as all structures will satisfy this condition based on our set-up (see Methods and Supplementary Methods for details). We compare SMINA and Vinardo scores against the experimental binding affinities using both RMSD filter types for the two scoring functions and cutoffs of 101 Angstroms, 100 Angstroms and 3 Angstroms (**Figure 2**). The sizes of the RefinedSet\CoreSet data satisfying the filters are provided in **Supplementary Table S1**.

The results indicate that the outputs of the docking tools consistently have a moderate correlation with the experimental results (on the order of 0.5), for both the RefinedSet\CoreSet, and the CoreSet. Upon restricting the Experimental RMSD cutoff, the Pearson correlation with the experimental docking scores (both SMINA and Vinardo) improves to 0.58-0.59 for the RefinedSet\CoreSet at RMSD < 100 Angstroms, while the correlation improves for the CoreSet only for RMSD < 3 Angstroms. The latter effect could be a result of either a legitimate increase in prediction quality when restricting the Experimental RMSD for the CoreSet, or could simply be the stochastic impact of a reduction in the dataset size. To test this, we ran Monte Carlo simulations randomly subsetting 197 out of 266 complexes a thousand times, and calculating the resulting correlation with experimental affinities. The empirical null distributions demonstrate that the improvement is unlikely to be a statistical artifact of subsampling (**Supplementary Figure S2B**). Overall, this indicates that constraining the pose to be similar to the experimental pose has benefits for the quality of the docking score prediction. The results for the Consensus RMSD do not suggest any significant improvement by lowering the RMSD cutoff (only a slight improvement is observed for the RefinedSet\CoreSet).

Additionally, it is interesting to note that the prediction on the CoreSet is consistently better than that of the RefinedSet\CoreSet. The most obvious explanation for this is that the scoring function for Vinardo was trained on the PDBbind 2013 CoreSet. This dataset overlaps with the PDBbind 2016 CoreSet we are using. The SMINA scoring function was trained on the CSAR-NRC HiQ 2010 data set⁹², which includes some structures from PDBbind RefinedSet from 2007. These overlaps will result in better performance on the CoreSet. Another possibility is that the complexes in the CoreSet are, by design, of a higher quality in terms of the removal of steric clashes and other structural irregularities relative to the RefinedSet\CoreSet. Working with such protein-ligand pairs may result in a better fit to the experimental binding affinities. We also note that the SMINA and Vinardo scores are highly correlated with each other, a fact that impacts meta-modeling later, as two strongly collinear features compete with each other when input into the same model.

We conclude that the overall performances of the docking results are not strong enough to make reliable predictions. The results motivated us to explore alternative methods of binding affinity prediction or scoring, especially deep learning tools.

Deep learning models

Trained models using BindingDB or PDBbind-RefinedSet

As our first group of DL models, we investigated either pre-trained (i.e., published) or *de novo*-trained models using the BindingDB (BDB) or PDBbind-RefinedSet (PDBb) data (model class D1, D2, or D3, respectively) (**Table 2**). Based on mean-squared-error (MSE), we selected the following top 6 out of the 12 *de novo*-trained models for subsequent analyses, which show comparable performance to the DeepPurpose pre-trained models with $MSE < 0.6$: CNN-CNN, Daylight-AAC, Morgan-AAC, Morgan-CNN, MPNN-CNN, and Transformer-CNN (**Supplementary Figure S3**). As the overlap between the published and *de novo*-trained models is only two, CNN-CNN and MPNN-CNN, this expanded the family of BDB-trained base models to a total of 10 with competitive performances in this study (**Table 2**). In terms of mean cross-validation (from 10x 5-fold CV), the best performing BDB-pre-trained, BDB-de-novo-trained, and PDBb-trained models were Daylight-AAC, Daylight-CNN, and CNN-AAC (**Table 2**). The model average Pearson correlation coefficients were 0.468, 0.475, and 0.746 for the CoreSet, respectively (**Figure 3A**; D1, D2, and D3). The two BDB-trained models perform worse than the docking tools (**Figure 2**). Full performance results are provided in **Supplementary Tables S2 and S3**. We note that the PDBb-trained models performed poorly for BDB-Kd predictions with no correlations (**Supplementary Figure S4**).

Fine-tuned models using PDBbind-RefinedSet

As our second group of models, we investigated fine-tuned models using PDBb for both BDB-pre-trained and BDB-de-novo-trained models (D1F and D2F, respectively). In terms of mean cross-validation (from 10x 5-fold CV), the best performing PDBb-finetuned models for BDB-pre-trained and BDB-de-novo-trained models were CNN-CNN and MPNN-AAC. The model average Pearson correlation coefficients were 0.716 and 0.749 for the CoreSet, respectively (**Figure 3A**). Full performance results are provided in **Supplementary Table S3**. As for BDB-Kd prediction, all PDBb-finetuned models maintained good performances with Pearson correlations of 0.6–0.7, compared to predictions by the BDB-trained models (**Supplementary Figures S4 and S5**).

PCA of predictions

As our third or final group of DL models, we investigated PCA projections of all predictions from those fine-tuned models for the BDB-pre-trained (D1F) or BDB-de-novo-trained (D2F) in the second model group ($6*5*10=300$ D1F or D2F model instances from 10x 5-fold CV for each model architecture) or those PDBb-trained models (D3) in the first model group ($10*5*10=500$ model instances). The first principal component (PC1) shows the best performance in all PCA, Pearson correlation coefficients for D1F, D2F, and D3 being 0.715, 0.749, and 0.747, respectively (**Figure 3A**; D1FP, D2FP, and D3P). We also performed PCA on the merged set of all predictions from D1F, D2F, and D3 ($300+300+500=1100$ model instances), the Pearson correlation coefficient for PC1 being 0.744 (**Figure 3A**; DAP). As expected, the PC1 is highly correlated with the mean prediction with the largest Pearson correlation coefficient of > 0.99 in all cases, while the second most correlated PC was not the second PC (PC2). By looking at performances of all cross-validated fine-tuned or PCA models, we observe that PC1 and D3 models tend to perform better than D1 or D2 models for the CoreSet in terms of Pearson correlation coefficients or mean squared errors (**Figure 3B**).

Comparisons among DL and docking models

Given that we have investigated the 38 DL models (6 D1, 6 D2, 10 D3, 6 D1F, 6 D2F, 1 D1FP, 1 D2FP, 1 D3P, and 1 DAP) as well as the 4 docking models, we first compared their predictions by Pearson correlation values among themselves. **Figure 4A** shows a heatmap of Pearson correlation values for all pairs of predictions for the CoreSet. As expected, high correlations (i.e., similar predictions) are observed among (1) the 4 docking models and (2) the fine-tuned or PC1 models (D1F, D2F, D1FP, D2FP, D3P). The BindingDB-based models (D1 and D2) are less correlated among themselves. Correlations between the experimental binding affinity and those predictions show that the top model is D1F|Daylight_AAC (pre-trained and fine-tuned) and the next top 3 models are PC1 models (**Figure 4B**). We also performed another comparison analysis by prediction errors or deviations from the experimental binding affinity (**Supplementary Table S3**). **Figures 4C** and **4D** show a heatmap and a box-whisker plot of prediction deviations or absolute errors for the 42 models. The fine-tuned or PC1 models tend to show lower errors than the BindingDB models, which in turn tend to show lower errors than the docking models. The top 5 models in terms of median errors are the 4 PC1 models and D2F|MPNN_Transformer (*de novo*-trained and fine-tuned). Similar but more pronounced correlations and deviations are observed for the training set, as expected (**Supplementary Figure S6**).

Meta-models of docking and DL tools

We ran several versions of meta-models to cover the spectrum of input features discussed in Methods (**Table 1**), with the goal of parsing the contributions of particular components of the models. The broad feature groups included docking scores, untransformed DL scores, and PC-transformed DL scores. Early exploratory analyses with SwissADME-derived ligand properties suggested the inclusion of molecular weight to contend with possible biases in the docking scores. Furthermore, we examined the impact of different DL training sets and models.

We present representative meta-model results using XGBoost in **Table 3** and **Fig. 5**, which showed the best performance among the 4 algorithms (**Supplementary Tables S4-S6**). The different panels show the scores for the XGBoost meta-models trained on RefinedSet\CoreSet in black and the corresponding test scores for the CoreSet in red. The panels of **Fig. 5** are arranged in a manner that reflects the different sets of features and training data: starting with meta-models constructed entirely based on the docking methods, SMINA and Vinardo; adding in MW; the inclusion of DL scores based on BindingDB or PDBbind trainings; and the fine-tuning and PCA. Note that, in the PC-based models, the optimal number of PCs was obtained by maximizing the respective machine-learning scores for a leave-out validation set (the RefinedSet\CoreSet was split 80%-20% into a training-validation partition).

We first note that the docking results alone (E) produce a moderate Pearson correlation for the test set (0.527). Unexpectedly, the E correlation for the training set (0.487) is lower than that for the test set. This might be due to the more careful curation and filtering of complexes in the CoreSet, relative to the broader RefinedSet\CoreSet. Moreover, adding in the molecular weight of the ligands (EW) showed significant improvements for both training and test sets. The original motivation for including the MW was the fact that the absolute deviation between the SMINA and Vinardo predictions and the experimental binding affinity is relatively highly correlated ($r \sim 0.3$) with the MW and a few related ADME features (such as the number of heavy atoms and molecular refractivity) than others (**Supplementary Table S7**). Including MW was an attempt at addressing this bias in the docking scores. We also noticed that the MW was correlated with the absolute deviation in the scores for some of the deep learning features, including the top principal component. When we added molecular weight as a meta-model feature (in all the

meta-models except for E), we found that the deviations of the final predictions are much less correlated with molecular weight (**Supplementary Table S8**).

In the next rows, it can be seen that the meta-models including DL scores significantly increase the Pearson correlation relative to the docking-based meta-models. The fine-tuning of the BindingDB-trained models on the PDBbind-RefinedSet\CoreSet improves the prediction performance. PCA on any of the DL scores improves performance even more. We note here that $D3$ was trained on the RefinedSet\CoreSet, while the $D1F$ and $D2F$ models were fine-tuned on the same set. This means that the training set for the DL training/fine-tuning process is identical to those for the associated meta-models ($ED1-F$, $ED1-F-P$, $ED2-F$, $ED2-F-P$, $ED3$, $ED3-P$, and $ED-A-P$). This also means that the leave-out validation split for the PC number optimization is not an independent dataset. The consequence of the most overlap between the DL and meta-model training sets is that we observe a very high correlation in the training set for those meta-models. Nonetheless, the high performances of these models on the external validation (CoreSet) signal good overall model robustness. The only caveat to this conclusion would stem from any systematic bias of the PDBbind dataset as a whole: if all the complexes in the full dataset were biased, then the use of a common training set would enable the models to learn the bias in the CoreSet as well, artificially inflating the performance. We are, however, not aware of any such bias in the PDBbind dataset, given that the complexes are sourced from a large number of independent studies.

Beneficial effects observed in the meta-models by performing PCA on the DL outputs are possibly due to the denoising or debiasing of outputs. The denoising is achieved by first running multiple parallel cross-validations, and then combining them into a lower-dimensional representation. However, unlike the DL results in **Fig. 3**, the performance improvement in the meta-models is not observed with the first PC alone, but rather requires the combination of a few PCs. We also note that, among the 4 PCA-based models ($ED1-F-P$, $ED2-F-P$, $ED3-P$, and $ED-A-P$), there are no large differences in the performance, i.e., different meta-model algorithms for PCA on different DL training processes show similar performances ($R = 0.76 - 0.78$). This suggests that we have maximized the information content of the constituent docking and DL model predictions.

To understand the contributions of the component features, we extracted the feature importance scores for each meta-model (**Supplementary Fig. S7**). We find that, while the contributions of the docking scores dominate for the EW , $ED1$, and $ED2$, these contributions drop to very low values for the other DL-containing meta-models. In all meta-models, SMINA scores contribute more than Vinardo scores. However, given the aforementioned similarity between the SMINA and Vinardo scores, this difference in the contributions between the two docking scores is more likely to be an artifact of the modeling process (and how it deals with nearly collinear features). The other noteworthy aspect of the importance scores is that the performance of $ED3$, fine-tuned, and PC-based meta-models is dominated by one, or at most two significant features. $ED1-F$, $ED2-F$ and $ED3$ are impacted mainly by two DL scores, while the PC models are dominated by PC1. We observe again that PC1 alone is not sufficient to improve the predictions, but requires the assistance of other PCs. The patterns of feature importance scores, however, are not entirely consistent across the different ML meta-models. The top features of the LASSO and Linear Regression meta-models are distinct from the XGBoost top features. The signed feature importance scores in the linear models show less domination of single scores, especially in the PC-based models. In particular, PC1, which is individually highly correlated with experimental binding affinities, is less important in the predictions by the linear meta-models. Given the similar performances of the ML meta-models, it appears that there are several paths to attaining nearly equivalent overall correlation values.

Given the improvement in the docking predictions by filtering out certain ligand-protein pairs (**Figs. 2** and **S1**), we explored the effect of the Experimental and Consensus RMSD filters with 3 and 100 Angstrom

cutoffs on the meta-models (**Supplementary Tables S4 and S5**). We found that the *E* and *EW* meta-models are affected by the different filters, with the Experimental RMSD filters producing slightly better results than the Consensus filters. This reinforces the idea that the docking affinity predictions benefit from constraining the predictions based on the pose. However, as the influence of the docking predictions decreases in the meta-models, it appears as if the impact of the RMSD filters also goes down and the best-performing meta-models show negligible difference in their performance with the various RMSD filters.

Prediction synergy and complementarity of docking and DL tools

As we obtained better overall performance by meta-modeling of docking and DL tools, we further investigated the degree of prediction synergy and complementarity of the two groups of tools, i.e., whether the meta-models utilize the strengths of both tool groups and the degree to which the two provide non-overlapping information. To do this, we focused on absolute errors of the mean predictions for the benchmark set by the 4 meta-models with ED-A-P, by the 4 docking tools, and by the DAP|PC1 model (**Fig. 4D**). When mutually compared, the mean predictions by the meta-models achieved the lowest errors for 123 of the 266 complexes (46.2%), the DAP|PC1 for 104 complexes (39.1%), and the docking tools for 39 complexes (14.7%) (**Figs. 6A-6C**). If we only compare the docking and DAP|PC1 tools, the former showed better mean predictions for 48 of the 266 complexes (18.0%) than the latter (**Fig. 6D**). This suggests that, beyond the globally better performance of the meta-models, prediction synergy is realized for 46.2% of the benchmark set by our meta-modeling due to complementary information of the docking and DL tools (even though each group of tools is better at predicting a subset of complexes by itself). Similarly, although the DL tools are generally better than the docking tools, there exists a small subset of complexes that are better predicted by the latter.

To further parse the differences between the outputs of the prediction tools, we assessed whether certain properties of the proteins or ligands are over- or under-represented in the complexes which were: (1) Best modeled by empirical docking; (2) Best modeled by deep learning; (3) Best modeled by meta-modeling. We also explored the top 50 complexes as predicted by the XGBoost Meta-model for ED-A-P to see if the performance of the meta-models relative to the experimental data was contingent on protein or ligand properties. We extracted protein features from the UniProt database and ligand features from the SwissADME database. We tested the significance of the occurrence of certain annotations (using Fisher’s exact test) and of the distributions of certain quantitative features (using a two-sided Wilcoxon test) for each of the four subsets of complexes. Specifically, we considered whether several UniProt features were annotated more or less frequently, and whether certain Gene Ontology (GO)⁹³, domain and pathway annotations occurred with different probabilities in the subsets. We also compared the distributions of the ligand SwissADME features. The results (**Supplementary Table S9**) indicate that there are practically no significant (nominal p-value ≤ 0.05) protein features prioritized in the four cases considered. This may be due to the fact that several proteins (and their associated UniProt IDs) are duplicated in the CoreSet. The number of reviewed proteins with UniProt IDs drops from 243 to 60 after removal of all duplicates. The highly significant results with nominal p-values ≤ 0.01 (both Wilcoxon and t-tests) are the distributions of several ligand features including MW, lipophilicity, and solubility measures in the structures for which the empirical docking tools perform the best. There is also some hint of significance for MW, the “#Rotatable bonds” and “#H-bond acceptors” in the structures for which the meta-models perform the best.

Comparison with structure-based tools

Having built our meta-models based on sequence-based DL models, we were interested in comparisons with structure-based tools through voxelization of binding pockets. We focus on the following 3 DL tools by re-training them with our training data for fair comparisons as much as possible as well as one recent tool based on advanced mathematics.

HAC-Net

A recent study developed a new structure-based DL ensemble or meta model, HAC-Net⁴⁷, by combining MP-GNN (message passing graph neural networks) and 3D-CNN (convolutional neural networks) trained on the PDBbind-2020 general set of >18,800 ligand-protein complexes. Their best performance was a Pearson correlation of 0.846 for the external data of the PDBbind-2016 CoreSet of 290 complexes. We note that we focused on the PDBbind-2020 RefinedSet rather than the general set because of two reasons: (1) higher quality and (2) limited resources. For a fairer, but limited, comparison, we re-trained HAC-Net with our training set of the PDBbind-2020 RefinedSet\CoreSet by subsetting from their train/validation/test data splits (4,942/82/265 out of 18,818/300/290 complexes from the general set, respectively). The Pearson correlation for the test set is 0.756, which is worse than our best meta-model performance of 0.777. Their MSE values are not comparable to ours because they used $-\log_{10}(K_d/K_i)$ while we used $\ln(K_d/K_i)$, which show different distributions of binding affinities for model training.

FAST

Jones et al. developed meta or fusion models, FAST⁴², by combining 3D-CNN and SG-CNN (spatial graph CNN). Due to technical difficulties, we were able to run their pre-trained SG-CNN model trained on the PDBbind-2016 general set excluding the CoreSet. We tested the model against the CoreSet of 266 complexes we used, which resulted in a Pearson correlation of 0.716, worse than HAC-Net. Their MSE is not comparable to ours for the same reason above.

KDeep

KDeep⁴⁶ was one of the earlier structure-based DL models with 3D-CNN to predict ligand-protein binding affinity. Their reported Pearson correlation on the PDBbind-2016 CoreSet was 0.82, which we were not able to verify because their code is not open-source. The KDeep model available on the public web-server could be re-trained with limited data size (KdeepTrainer, <https://playmolecule.com/KdeepTrainer/>). While we were not able to use our full training data due to the limitation, we were able to re-train the KDeep model for 250 epochs with each of 3 training sets of random 1,800 complexes sampled from our training set of the PDBbind-2020 RefinedSet. We then tested the 3 trained models against the CoreSet we used. We obtained Pearson correlations of 0.718–0.766, which are similar to those reported values of 0.701–0.738 by Kwon et al. using the PDBbind-2016 RefinedSet as a training set and 4 different learning rates⁵⁰.

PerSpect ML

PerSpect ML⁶⁹ is one of the best performing tools in recent years, which reported the highest Pearson correlation of 0.84 in the case of the PDBbind 2016 CoreSet. It is based on topological data analysis and spectral theory for multiscale molecular featurization, which provided a feature set for the gradient boosting tree-based regression. While there was a technical difficulty, due to incomplete code availability, to reproduce or implement PerSpect ML for fair comparisons with the data we used, those recent methods based on advanced mathematics from the Xia group⁶⁷⁻⁷⁰ showed largely better performances than ours

and others. We note, however, that they may generate more than 100,000 features requiring 3D structures or binding poses, which are often unavailable in real-world drug discovery.

Despite those limited comparisons, we conclude that our meta-models or our sequence-based DL models show competitive performances or advantages to more sophisticated structure-based models.

Virtual screening benchmark

To further explore the performance of the models on specific target proteins with multiple ligands, we designed a virtual screening benchmark against 3 target proteins for 35 complexes from the PDBbind v2020 GeneralSet: O60341, O15151, and P0C6U8 (see Methods). The performances of our models for the 3 target proteins are shown in **Table 4** in comparison with the 3 tools described above, HAC-Net (re-trained), SG-CNN (FAST; pre-trained), and KDeep (the up-to-date default version on their web server). The pre-trained SG-CNN performed best for O60341 and O15151 in terms of RMSE (2.10 and 1.37, respectively). This was expected because their training data were the PDBbind v2016 GeneralSet, which includes 30 out of the 35 complexes in our benchmark set except 5 complexes for O60341. Otherwise, our meta-models or fine-tuned DL models performed best for all 3 target proteins in terms of both RMSE and Pearson’s correlation. Our best performing models are ED2-F_VvS_101.0_LinReg (meta-model; docking + MW + de novo-trained & fine-tuned DL by linear regression) and D1F|Daylight_AAC (pre-trained & fine-tuned DL model) for O60341 (RMSE = 2.34), EW_VvS_101.0_LinReg (meta-model; docking + MW by linear regression) for O15151 (RMSE = 1.44), and D2F|MPNN-AAC (de novo-trained & fine-tuned DL model) for P0C6U8 (RMSE = 1.01). We consider the Pearson correlation metric less reliable due to the small sample size.

As noted in the previous section on prediction synergy, different meta-models or component DL/docking models may perform best for different complexes or proteins. In the case of this virtual screening, we noticed that while some of the same meta-models would often predict the binding affinities for O60341 and P0C6U8 with reasonable accuracy, they would not predict the affinities for O15151 as well, and vice versa. For example, ED2-F_VvS_101.0_LinReg showed low RMSEs for O60341 (RMSE = 2.34) and P0C6U8 (RMSE = 2.54) but higher RMSEs for O15151 (RMSE = 5.88). In particular, we observe that 6 out of the 8 ligands in the complexes for O15151 were k-mers ($k = 10, 12, \text{ or } 15$) with relatively high MW of >1000 . Among the 35 complexes there are 18 k-mers with mean MW of 927.2 compared to 762.7 for 17 non-k-mers. We note that about 5% of the RefinedSet (we used for model training) and about 10% of the GeneralSet contain k-mers (up to 10-mer and 19-mer, respectively). Given that k-mers are not representative and tend to have high MW, we aimed to assess whether high or low MW causes differences in the performance of the meta-models independently from the choice of a target protein by dividing ligands into two groups of low MW ≤ 900 and high MW > 900 (the median threshold for the 35 complexes). By focusing on ED2-F_VvS_101.0_LinReg from above, we find that the accuracy for low MW ligands is better than high MW ligands (RMSE = 2.45 vs. 4.36). This is expected given the fact that the ligands in the RefinedSet we used for training have mean MW of 384.3 and standard deviation of 172.6 and that the Pearson correlations between predictions and MW are negative ranging from -0.62 to -0.29. While far from conclusive for generalization, these results suggest that there might be identifiable features of ligands and/or proteins which would explain why certain meta-models perform variably for different target proteins.

Although the above results suggest that top-ranking high-affinity ligands predicted by our models could be prioritized as hits in virtual screening, we also tested our models using the virtual screening benchmark dataset of LIT-PCBA to distinguish 10 active ligands from 10 inactive ligands for 15 proteins (see **Methods; Supplementary Table S10**). As our models were not trained for binary classification of active and inactive ligands, our hypothesis was that active ligands tend to have higher affinity scores than

inactive ligands. To test the hypothesis, we evaluated the fraction of active ligands in the 5 highest-scoring ligands for each protein (**Table 5**) and the distribution difference of predicted affinity scores between 10 active and 10 inactive ligands for each protein (Wilcoxon and Mann-Whitney U tests; **Supplementary Table S11**). The results show that our 5 highest-scoring ligands by either averaged DL models or averaged meta-models tend to be active ligands (i.e., >50%) for 11 out of the 15 proteins and that active ligands tend to have higher affinity scores than inactive ligands for most of the proteins. We also observe that our DL models and meta-models tend to predict higher fractions of active ligands (>=80%) than the baseline docking tools, SMINA or Vinardo (**Table 5**). Specifically, all the top 5 predicted ligands by D3|Transformer-CNN are active ligands for all the 15 proteins. More than 50% of the top 5 predicted ligands by most of the EW meta-models are active ligands for 13 out of the 15 proteins. We note, however, that, as in the section on prediction synergy, there is variability among the target proteins in terms of the best-performing model. Different protein targets may benefit from the use of different modeling techniques, conditional on their physicochemical properties. This is also observed in terms of the target-specific behavior of the p-values (**Supplementary Table S11**).

Overall, we conclude that the family of our models are competitive to several state-of-the-art structure-based models and also useful for virtual screening applications.

Discussion

The framework we present here, inspired by stacked generalization and super learner^{74, 75}, is based on the central concept that different models designed and trained for the same prediction task often carry model-specific biases. Hence, simple approaches to combining the results of their independent predictions may yield superior results if the biases are even partially independent and the models are complementary to some degree. Indeed, we find this to be borne out in the ligand-protein binding affinity prediction in several ways. First, we find that combining the predictions from empirical docking methods with those from the pre-trained or *de novo*-trained deep learning tools can yield gains in predictive power over the individual approaches (ED1-3 vs. E or D1-2). Second, utilizing models trained on the BindingDB as the base and refining them on the PDBbind resulted in significant improvements (D1 and D2 vs. D1F and D2F, respectively), demonstrating that fine-tuning pre-trained models could retain good predictive quality on both primary (BindingDB) and secondary (PDBbind) datasets (**Supplementary Fig. S4**). Third, even within the suite of deep learning tools, transforming their prediction scores through principal component analysis could improve the performance on the test set (i.e., principal component regression). This may be due to a de-noising of individual DL scores. Finally, in addition to performance improvement or synergy by the meta-models over the docking and DL models for a subset of complexes, the use of meta-models by canonical machine learning enables us to explicitly add features that may be associated with prediction deviations in the individual models. For example, we found that, for both empirical docking tools and some deep learning models, the deviations of the predictions from the experimental affinities were correlated with molecular weight. Explicitly adding in molecular weight as a meta-model feature resulted in the deviations of the final predictions being much less correlated with molecular weight.

Overall, our framework corroborates existing work on ensemble learning, stacked generalization, super learner, and consensus-based improvements in predictions. Our machine-learning-based meta-models allow for the flexibility of adding or removing any component tools, physicochemical properties, or molecular descriptors as part of feature engineering. Models trained on multiple datasets (e.g. BindingDB and PDBbind) and on multiple data types (e.g. sequence and/or structure) may be unified to reduce individual biases and improve predictions. Furthermore, we posit that the DL models from DeepPurpose considered herein, being sequence-based, offer better scalability. Given that only ligand and protein sequences are required for the prediction, and not all-atom 3D structures, we expect that increasingly large databases could be used for training in future iterations by running high-throughput experimental binding affinity assays (without the need for concurrent X-ray or NMR experiments) as a filtering strategy in early drug discovery. Considering that the observed performances of these models for both benchmarks of CASF-2016 and the small-scale virtual screening are better or on par with more sophisticated structure-based DL models, there is an argument to be made in favor of more scalable approaches. Additionally, we note that the public and private experimental binding affinity databases are highly fragmented, in that they are produced separately, with potentially different types of assays, or at different scales. While efforts such as the PDBbind database manage to carefully curate a high-quality single dataset, not all data sources can be incorporated because of the type of data (e.g. experimental data without associated structures being available) or because of data access (e.g. behind a private paywall). Our meta-modeling may address some of these issues by pooling only prediction outputs from models trained on diverse public or private databases with or without available structures, protecting the databases themselves if necessary and maintaining performance quality. Subsequent in-depth analysis could also identify prediction synergy and complementarity of all available tools as we demonstrated in **Fig. 6**. Finally, there might be value in expanding families of meta-models with different input data, each family being optimized to target a particular protein or class of proteins and/or ligands as demonstrated in **Tables 4 and 5**.

We acknowledge some limitations of our study. First, we primarily focused on a single dataset, PDBbind

RefinedSet, for both training and testing. In fact, in light of recent positive results from training models on the full PDBbind General Set of ~19,000 complexes^{42, 47}, there is a scope for further scale-up of the model training process with larger data. It is worth mentioning, however, that when Jones et al. used the PDBbind general or refined set for model training, they observed the tradeoffs between data quality and quantity in performance of different models: SG-CNN performed better with the general set (in favor of data quantity); 3D-CNN performed better with the refined set (in favor of data quality). On the other hand, we started with DL models pre-trained on BindingDB of ~66,000 complexes and either employed them “out of the box” or fine-tuned them on the PDBbind RefinedSet (excluding the CoreSet). The two BindingDB-based meta-models, ED1 and ED2, perform better than any of the stand-alone docking or DL tools (Pearson correlation 0.62-0.64 vs. 0.47-0.59). We also tested the two PDBbind fine-tuned models, D1F and D2F, on the primary training set of BindingDB, to ascertain the degree to which the models retained their “out of the box” performance on the primary training set. We found reasonably good correlations for D1F and D2F ($r = 0.636$ to 0.711) (**Supplementary Fig. S4**) compared to the pre-trained D1 ($r = 0.8$)⁵⁷. However, the PDBbind-trained D3 showed poor prediction on BindingDB ($r < 0.2$). More importantly, while the CASF-2016 benchmark set has been well accepted, more benchmark sets of high quality would be needed to test and compare models in a more objective manner and also to challenge model generalization. Our virtual screening benchmarks are also very limited and our models tend to perform well for ligands with low molecular weight. In particular, the binary classification problem for screening of active or functional ligands would require a new model development for higher accuracy rather than repurposing exclusively affinity-based regression models as in this study. In this sense, the good performances of our fine-tuned DL models or meta-models do not imply model generalizability. We also note that we neither fine-tuned the docking tools nor conducted hyperparameter optimization for the DL models, which might help performance as well.

Our proof-of-concept study of meta-modeling can be readily extended to integrate with (i.e., to add more meta features of) predictions from any other tools, such as HAC-Net, FAST, KDeep, and/or PerSpect ML, molecular properties or embeddings, or even predictions from the same base models trained on different orthogonal datasets, to address model bias and robustness, which is the key conceptual advantage of any ensemble or fusion model. In parallel to this type of horizontal extension (i.e., feature engineering), it is conceivable that meta-models may be expanded or stacked vertically, leading to deep meta-models. Our meta-modeling approach offers promising and flexible strategies for future model iterations to further improve ligand-protein binding affinity prediction.

Data and code availability

The BindingDB and PDBbind databases are publicly available. The code is available on our GitHub page at <https://github.com/Lee1701/Lee2023a>.

Supporting Information

Supporting Information contains supplementary methods, supplementary figures, and supplementary references.

Acknowledgements

We thank the Yale Center for Research Computing for their high-performance-computing resources and help. We also thank Drs. Jeffrey Brock and Sarah Miller for their support in the initiation of this project through the COVID HASTE community at the Yale School of Engineering & Applied Science.

Author contributions

HL and PSE conceived, designed, and performed the study, analyzed the data, and drafted the manuscript. HL, PSE, and MGB interpreted the data and critically reviewed and approved the manuscript. HL supervised the study.

Competing interests

HL reports a consulting role at Guidepoint outside of this submitted work. The other authors report no competing interests.

References

1. Shen, C.; Ding, J.; Wang, Z.; Cao, D.; Ding, X.; Hou, T., From machine learning to deep learning: Advances in scoring functions for protein–ligand docking. *WIREs Computational Molecular Science* **2020**, *10*, e1429.
2. Ain, Q. U.; Aleksandrova, A.; Roessler, F. D.; Ballester, P. J., Machine-learning scoring functions to improve structure-based binding affinity prediction and virtual screening. *Wiley Interdiscip Rev Comput Mol Sci* **2015**, *5*, 405-424.
3. Khamis, M. A.; Gomaa, W.; Ahmed, W. F., Machine learning in computational docking. *Artif Intell Med* **2015**, *63*, 135-52.
4. Kitchen, D. B.; Decornez, H.; Furr, J. R.; Bajorath, J., Docking and scoring in virtual screening for drug discovery: methods and applications. *Nat Rev Drug Discov* **2004**, *3*, 935-49.
5. Moitessier, N.; Englebienne, P.; Lee, D.; Lawandi, J.; Corbeil, C. R., Towards the development of universal, fast and highly accurate docking/scoring methods: a long way to go. *Br J Pharmacol* **2008**, *153* Suppl 1, S7-26.
6. Grinter, S. Z.; Zou, X., Challenges, applications, and recent advances of protein-ligand docking in structure-based drug design. *Molecules* **2014**, *19*, 10150-76.
7. Su, M.; Yang, Q.; Du, Y.; Feng, G.; Liu, Z.; Li, Y.; Wang, R., Comparative Assessment of Scoring Functions: The CASF-2016 Update. *J Chem Inf Model* **2019**, *59*, 895-913.
8. Ferreira, L. G.; Dos Santos, R. N.; Oliva, G.; Andricopulo, A. D., Molecular docking and structure-based drug design strategies. *Molecules* **2015**, *20*, 13384-421.
9. Sousa, S. F.; Fernandes, P. A.; Ramos, M. J., Protein-ligand docking: current status and future challenges. *Proteins* **2006**, *65*, 15-26.
10. Krovat, M. E.; Steindl, T.; Langer, T., Recent Advances in Docking and Scoring. *Current Computer-Aided Drug Design* **2005**, *1*, 93-102.
11. Ballester, P. J.; Mitchell, J. B. O., A machine learning approach to predicting protein–ligand binding affinity with applications to molecular docking. *Bioinformatics* **2010**, *26*, 1169-1175.
12. Böhm, H. J., The development of a simple empirical scoring function to estimate the binding constant for a protein-ligand complex of known three-dimensional structure. *J Comput Aided Mol Des* **1994**, *8*, 243-56.
13. Ruvinsky, A. M., Role of binding entropy in the refinement of protein-ligand docking predictions: analysis based on the use of 11 scoring functions. *J Comput Chem* **2007**, *28*, 1364-72.
14. Mysinger, M. M.; Shoichet, B. K., Rapid context-dependent ligand desolvation in molecular docking. *J Chem Inf Model* **2010**, *50*, 1561-73.
15. Lill, M. A., Efficient incorporation of protein flexibility and dynamics into molecular docking simulations. *Biochemistry* **2011**, *50*, 6157-69.
16. Cheng, T.; Li, X.; Li, Y.; Liu, Z.; Wang, R., Comparative Assessment of Scoring Functions on a Diverse Test Set. *Journal of Chemical Information and Modeling* **2009**, *49*, 1079-1093.
17. Wang, R.; Lu, Y.; Fang, X.; Wang, S., An Extensive Test of 14 Scoring Functions Using the PDBbind Refined Set of 800 Protein–Ligand Complexes. *Journal of Chemical Information and Computer Sciences* **2004**, *44*, 2114-2125.
18. Warren, G. L.; Andrews, C. W.; Capelli, A. M.; Clarke, B.; LaLonde, J.; Lambert, M. H.; Lindvall, M.; Nevins, N.; Semus, S. F.; Senger, S.; Tedesco, G.; Wall, I. D.; Woolven, J. M.; Peishoff, C. E.; Head, M. S., A critical assessment of docking programs and scoring functions. *J Med Chem* **2006**, *49*, 5912-31.
19. Trott, O.; Olson, A. J., AutoDock Vina: improving the speed and accuracy of docking with a new scoring function, efficient optimization, and multithreading. *J Comput Chem* **2010**, *31*, 455-61.
20. Koes, D. R.; Baumgartner, M. P.; Camacho, C. J., Lessons learned in empirical scoring with smina from the CSAR 2011 benchmarking exercise. *J Chem Inf Model* **2013**, *53*, 1893-904.

21. Wang, R.; Wang, S., How does consensus scoring work for virtual library screening? An idealized computer experiment. *J Chem Inf Comput Sci* **2001**, *41*, 1422-6.
22. Charifson, P. S.; Corkery, J. J.; Murcko, M. A.; Walters, W. P., Consensus scoring: A method for obtaining improved hit rates from docking databases of three-dimensional structures into proteins. *J Med Chem* **1999**, *42*, 5100-9.
23. Houston, D. R.; Walkinshaw, M. D., Consensus Docking: Improving the Reliability of Docking in a Virtual Screening Context. *Journal of Chemical Information and Modeling* **2013**, *53*, 384-390.
24. Palacio-Rodríguez, K.; Lans, I.; Cavasotto, C. N.; Cossio, P., Exponential consensus ranking improves the outcome in docking and receptor ensemble docking. *Scientific Reports* **2019**, *9*, 5142.
25. Liu, Z.; Su, M.; Han, L.; Liu, J.; Yang, Q.; Li, Y.; Wang, R., Forging the Basis for Developing Protein-Ligand Interaction Scoring Functions. *Accounts of Chemical Research* **2017**, *50*, 302-309.
26. Ashtawy, H. M.; Mahapatra, N. R., A Comparative Assessment of Ranking Accuracies of Conventional and Machine-Learning-Based Scoring Functions for Protein-Ligand Binding Affinity Prediction. *IEEE/ACM Trans. Comput. Biol. Bioinformatics* **2012**, *9*, 1301-1313.
27. Patel, L.; Shukla, T.; Huang, X.; Ussery, D. W.; Wang, S., Machine Learning Methods in Drug Discovery. *Molecules* **2020**, *25*.
28. Wójcikowski, M.; Ballester, P. J.; Siedlecki, P., Performance of machine-learning scoring functions in structure-based virtual screening. *Sci Rep* **2017**, *7*, 46710.
29. Baum, B.; Muley, L.; Smolinski, M.; Heine, A.; Hangauer, D.; Klebe, G., Non-additivity of functional group contributions in protein-ligand binding: a comprehensive study by crystallography and isothermal titration calorimetry. *J Mol Biol* **2010**, *397*, 1042-54.
30. Baskin, II; Winkler, D.; Tetko, I. V., A renaissance of neural networks in drug discovery. *Expert Opin Drug Discov* **2016**, *11*, 785-95.
31. Dana, D.; Gadhiya, S. V.; St Surin, L. G.; Li, D.; Naaz, F.; Ali, Q.; Paka, L.; Yamin, M. A.; Narayan, M.; Goldberg, I. D.; Narayan, P., Deep Learning in Drug Discovery and Medicine; Scratching the Surface. *Molecules* **2018**, *23*.
32. Sapoval, N.; Aghazadeh, A.; Nute, M. G.; Antunes, D. A.; Balaji, A.; Baraniuk, R.; Barberan, C. J.; Dannenfeler, R.; Dun, C.; Edrisi, M.; Elworth, R. A. L.; Kille, B.; Kyrillidis, A.; Nakhleh, L.; Wolfe, C. R.; Yan, Z.; Yao, V.; Treangen, T. J., Current progress and open challenges for applying deep learning across the biosciences. *Nature Communications* **2022**, *13*, 1728.
33. Yang, Z.; Zeng, X.; Zhao, Y.; Chen, R., AlphaFold2 and its applications in the fields of biology and medicine. *Signal Transduction and Targeted Therapy* **2023**, *8*, 115.
34. Akdel, M.; Pires, D. E. V.; Pardo, E. P.; Jänes, J.; Zalevsky, A. O.; Mészáros, B.; Bryant, P.; Good, L. L.; Laskowski, R. A.; Pozzati, G.; Shenoy, A.; Zhu, W.; Kundrotas, P.; Serra, V. R.; Rodrigues, C. H. M.; Dunham, A. S.; Burke, D.; Borkakoti, N.; Velankar, S.; Frost, A.; Basquin, J.; Lindorff-Larsen, K.; Bateman, A.; Kajava, A. V.; Valencia, A.; Ovchinnikov, S.; Durairaj, J.; Ascher, D. B.; Thornton, J. M.; Davey, N. E.; Stein, A.; Elofsson, A.; Croll, T. I.; Beltrao, P., A structural biology community assessment of AlphaFold2 applications. *Nature Structural & Molecular Biology* **2022**, *29*, 1056-1067.
35. Abbasi, K.; Razzaghi, P.; Poso, A.; Ghanbari-Ara, S.; Masoudi-Nejad, A., Deep Learning in Drug Target Interaction Prediction: Current and Future Perspectives. *Curr Med Chem* **2021**, *28*, 2100-2113.
36. Li, H.; Zou, L.; Kowah, J. A. H.; He, D.; Liu, Z.; Ding, X.; Wen, H.; Wang, L.; Yuan, M.; Liu, X., A compact review of progress and prospects of deep learning in drug discovery. *J Mol Model* **2023**, *29*, 117.
37. Kim, J.; Park, S.; Min, D.; Kim, W., Comprehensive Survey of Recent Drug Discovery Using Deep Learning. *Int J Mol Sci* **2021**, *22*.
38. Lavecchia, A., Deep learning in drug discovery: opportunities, challenges and future prospects. *Drug Discov Today* **2019**, *24*, 2017-2032.
39. Ma, J.; Sheridan, R. P.; Liaw, A.; Dahl, G. E.; Svetnik, V., Deep Neural Nets as a Method for

- Quantitative Structure–Activity Relationships. *Journal of Chemical Information and Modeling* **2015**, *55*, 263–274.
40. Krizhevsky, A.; Sutskever, I.; Hinton, G. E., ImageNet classification with deep convolutional neural networks. In *Proceedings of the 25th International Conference on Neural Information Processing Systems - Volume 1*, Curran Associates Inc.: Lake Tahoe, Nevada, 2012; pp 1097–1105.
41. Szegedy, C.; Liu, W.; Jia, Y.; Sermanet, P.; Reed, S.; Anguelov, D.; Erhan, D.; Vanhoucke, V.; Rabinovich, A. Going Deeper with Convolutions 2014, p. arXiv:1409.4842.
<https://ui.adsabs.harvard.edu/abs/2014arXiv1409.4842S> (accessed September 01, 2014).
42. Jones, D.; Kim, H.; Zhang, X.; Zemla, A.; Stevenson, G.; Bennett, W. F. D.; Kirshner, D.; Wong, S. E.; Lightstone, F. C.; Allen, J. E., Improved Protein–Ligand Binding Affinity Prediction with Structure-Based Deep Fusion Inference. *Journal of Chemical Information and Modeling* **2021**, *61*, 1583–1592.
43. Gomes, J.; Ramsundar, B.; Feinberg, E. N.; Pande, V. S. Atomic Convolutional Networks for Predicting Protein-Ligand Binding Affinity 2017, p. arXiv:1703.10603.
<https://ui.adsabs.harvard.edu/abs/2017arXiv170310603G> (accessed March 01, 2017).
44. Wallach, I.; Dzamba, M.; Heifets, A. AtomNet: A Deep Convolutional Neural Network for Bioactivity Prediction in Structure-based Drug Discovery 2015, p. arXiv:1510.02855.
<https://ui.adsabs.harvard.edu/abs/2015arXiv151002855W> (accessed October 01, 2015).
45. Ragoza, M.; Hochuli, J.; Idrobo, E.; Sunseri, J.; Koes, D. R., Protein–Ligand Scoring with Convolutional Neural Networks. *Journal of Chemical Information and Modeling* **2017**, *57*, 942–957.
46. Jiménez, J.; Škalič, M.; Martínez-Rosell, G.; De Fabritiis, G., KDEEP: Protein–Ligand Absolute Binding Affinity Prediction via 3D-Convolutional Neural Networks. *Journal of Chemical Information and Modeling* **2018**, *58*, 287–296.
47. Kyro, G. W.; Brent, R. I.; Batista, V. S., HAC-Net: A Hybrid Attention-Based Convolutional Neural Network for Highly Accurate Protein–Ligand Binding Affinity Prediction. *Journal of Chemical Information and Modeling* **2023**, *63*, 1947–1960.
48. Wang, Z.; Zheng, L.; Liu, Y.; Qu, Y.; Li, Y.-Q.; Zhao, M.; Mu, Y.; Li, W., OnionNet-2: A Convolutional Neural Network Model for Predicting Protein-Ligand Binding Affinity Based on Residue-Atom Contacting Shells. *Frontiers in Chemistry* **2021**, *9*.
49. Shan, W.; Li, X.; Yao, H.; Lin, K., Convolutional Neural Network-based Virtual Screening. *Curr Med Chem* **2021**, *28*, 2033–2047.
50. Kwon, Y.; Shin, W.-H.; Ko, J.; Lee, J., AK-Score: Accurate Protein-Ligand Binding Affinity Prediction Using an Ensemble of 3D-Convolutional Neural Networks. *International Journal of Molecular Sciences* **2020**, *21*, 8424.
51. Jiang, H.; Wang, J.; Cong, W.; Huang, Y.; Ramezani, M.; Sarma, A.; Dokholyan, N. V.; Mahdavi, M.; Kandemir, M. T., Predicting Protein-Ligand Docking Structure with Graph Neural Network. *J Chem Inf Model* **2022**, *62*, 2923–2932.
52. Knutson, C.; Bontha, M.; Billbrey, J. A.; Kumar, N., Decoding the protein-ligand interactions using parallel graph neural networks. *Sci Rep* **2022**, *12*, 7624.
53. Nikolaienko, T.; Gurbych, O.; Druchok, M., Complex machine learning model needs complex testing: Examining predictability of molecular binding affinity by a graph neural network. *J Comput Chem* **2022**, *43*, 728–739.
54. Yang, Z.; Zhong, W.; Lv, Q.; Dong, T.; Yu-Chian Chen, C., Geometric Interaction Graph Neural Network for Predicting Protein-Ligand Binding Affinities from 3D Structures (GIGN). *J Phys Chem Lett* **2023**, *14*, 2020–2033.
55. Feinberg, E. N.; Sur, D.; Wu, Z.; Husic, B. E.; Mai, H.; Li, Y.; Sun, S.; Yang, J.; Ramsundar, B.; Pande, V. S., PotentialNet for Molecular Property Prediction. *ACS Cent Sci* **2018**, *4*, 1520–1530.

56. Karlov, D. S.; Sosnin, S.; Fedorov, M. V.; Popov, P., graphDelta: MPNN Scoring Function for the Affinity Prediction of Protein-Ligand Complexes. *ACS Omega* **2020**, *5*, 5150-5159.
57. Huang, K.; Fu, T.; Glass, L.; Zitnik, M.; Xiao, C.; Sun, J., DeepPurpose: a Deep Learning Library for Drug-Target Interaction Prediction and Applications to Repurposing and Screening. *arXiv* **2020**, *2004.08919*.
58. Öztürk, H.; Özgür, A.; Ozkirimli, E., DeepDTA: deep drug-target binding affinity prediction. *Bioinformatics* **2018**, *34*, i821-i829.
59. Castelvechi, D., Can we open the black box of AI? *Nature* **2016**, *538*, 20-23.
60. Doshi-Velez, F.; Kim, B., Towards a rigorous science of interpretable machine learning. *arXiv preprint arXiv:1702.08608* **2017**.
61. Murdoch, W. J.; Singh, C.; Kumbier, K.; Abbasi-Asl, R.; Yu, B., Definitions, methods, and applications in interpretable machine learning. *Proceedings of the National Academy of Sciences* **2019**, *116*, 22071-22080.
62. Barredo Arrieta, A.; Díaz-Rodríguez, N.; Del Ser, J.; Bennetot, A.; Tabik, S.; Barbado, A.; Garcia, S.; Gil-Lopez, S.; Molina, D.; Benjamins, R.; Chatila, R.; Herrera, F., Explainable Artificial Intelligence (XAI): Concepts, taxonomies, opportunities and challenges toward responsible AI. *Information Fusion* **2020**, *58*, 82-115.
63. Roscher, R.; Bohn, B.; Duarte, M. F.; Garcke, J., Explainable Machine Learning for Scientific Insights and Discoveries. *IEEE Access* **2020**, *8*, 42200-42216.
64. Cang, Z.; Wei, G. W., Integration of element specific persistent homology and machine learning for protein-ligand binding affinity prediction. *Int J Numer Method Biomed Eng* **2018**, *34*.
65. Cang, Z.; Mu, L.; Wei, G. W., Representability of algebraic topology for biomolecules in machine learning based scoring and virtual screening. *PLoS Comput Biol* **2018**, *14*, e1005929.
66. Wu, J.; Chen, H.; Cheng, M.; Xiong, H., CurvAGN: Curvature-based Adaptive Graph Neural Networks for Predicting Protein-Ligand Binding Affinity. *BMC Bioinformatics* **2023**, *24*, 378.
67. Wee, J.; Xia, K., Ollivier Persistent Ricci Curvature-Based Machine Learning for the Protein-Ligand Binding Affinity Prediction. *Journal of Chemical Information and Modeling* **2021**, *61*, 1617-1626.
68. Wee, J.; Xia, K., Forman persistent Ricci curvature (FPRC)-based machine learning models for protein-ligand binding affinity prediction. *Briefings in Bioinformatics* **2021**, *22*.
69. Meng, Z.; Xia, K., Persistent spectral-based machine learning (PerSpect ML) for protein-ligand binding affinity prediction. *Science Advances* **2021**, *7*, eabc5329.
70. Liu, X.; Feng, H.; Wu, J.; Xia, K., Persistent spectral hypergraph based machine learning (PSH-ML) for protein-ligand binding affinity prediction. *Briefings in Bioinformatics* **2021**, *22*.
71. Nguyen, D. D.; Gao, K.; Wang, M.; Wei, G.-W., MathDL: mathematical deep learning for D3R Grand Challenge 4. *Journal of Computer-Aided Molecular Design* **2020**, *34*, 131-147.
72. Moon, S.; Zhung, W.; Yang, S.; Lim, J.; Kim, W. Y., PIGNet: a physics-informed deep learning model toward generalized drug-target interaction predictions. *Chemical Science* **2022**, *13*, 3661-3673.
73. Guedes, I. A.; Barreto, A. M. S.; Marinho, D.; Krempser, E.; Kuenemann, M. A.; Sperandio, O.; Dardenne, L. E.; Miteva, M. A., New machine learning and physics-based scoring functions for drug discovery. *Scientific Reports* **2021**, *11*, 3198.
74. Wolpert, D. H., Stacked generalization. *Neural Networks* **1992**, *5*, 241-259.
75. Laan, M. J. v. d.; Polley, E. C.; Hubbard, A. E., Super Learner. *Statistical Applications in Genetics and Molecular Biology* **2007**, *6*.
76. Bennett, J.; Elkan, C.; Liu, B.; Smyth, P.; Tikk, D., KDD Cup and workshop 2007. *SIGKDD Explor. Newsl.* **2007**, *9*, 51-52.
77. Feuerverger, A.; He, Y.; Khatri, S., Statistical Significance of the Netflix Challenge. *Statistical Science* **2012**, *27*, 202-231, 30.

78. Hallinan, B.; Striphas, T., Recommended for you: The Netflix Prize and the production of algorithmic culture. *New Media & Society* **2016**, *18*, 117-137.
79. Bell, R. M.; Koren, Y.; Volinsky, C., All Together Now: A Perspective on the Netflix Prize. *CHANCE* **2010**, *23*, 24-29.
80. Reichstein, M.; Camps-Valls, G.; Stevens, B.; Jung, M.; Denzler, J.; Carvalhais, N.; Prabhat, Deep learning and process understanding for data-driven Earth system science. *Nature* **2019**, *566*, 195-204.
81. Karniadakis, G. E.; Kevrekidis, I. G.; Lu, L.; Perdikaris, P.; Wang, S.; Yang, L., Physics-informed machine learning. *Nature Reviews Physics* **2021**, *3*, 422-440.
82. Thuerey, N.; Holl, P.; Mueller, M.; Schnell, P.; Trost, F.; Um, K., Physics-based Deep Learning. *ArXiv* **2021**, *abs/2109.05237*.
83. Wang, B.; Yan, C.; Lou, S.; Emani, P.; Li, B.; Xu, M.; Kong, X.; Meyerson, W.; Yang, Y. T.; Lee, D.; Gerstein, M., Building a Hybrid Physical-Statistical Classifier for Predicting the Effect of Variants Related to Protein-Drug Interactions. *Structure* **2019**, *27*, 1469-1481.e3.
84. Gilson, M. K.; Liu, T.; Baitaluk, M.; Nicola, G.; Hwang, L.; Chong, J., BindingDB in 2015: A public database for medicinal chemistry, computational chemistry and systems pharmacology. *Nucleic Acids Research* **2015**, *44*, D1045-D1053.
85. Li, Y.; Han, L.; Liu, Z.; Wang, R., Comparative Assessment of Scoring Functions on an Updated Benchmark: 2. Evaluation Methods and General Results. *Journal of Chemical Information and Modeling* **2014**, *54*, 1717-1736.
86. Quiroga, R.; Villarreal, M. A., Vinardo: A Scoring Function Based on Autodock Vina Improves Scoring, Docking, and Virtual Screening. *PLoS One* **2016**, *11*, e0155183.
87. Blanes-Mira, C.; Fernández-Aguado, P.; de Andrés-López, J.; Fernández-Carvajal, A.; Ferrer-Montiel, A.; Fernández-Ballester, G., Comprehensive Survey of Consensus Docking for High-Throughput Virtual Screening. *Molecules* **2023**, *28*, 175.
88. Daina, A.; Michielin, O.; Zoete, V., SwissADME: a free web tool to evaluate pharmacokinetics, drug-likeness and medicinal chemistry friendliness of small molecules. *Scientific Reports* **2017**, *7*, 42717.
89. The UniProt Consortium, UniProt: the Universal Protein Knowledgebase in 2023. *Nucleic Acids Res* **2023**, *51*, D523-d531.
90. Camacho, C.; Coulouris, G.; Avagyan, V.; Ma, N.; Papadopoulos, J.; Bealer, K.; Madden, T. L., BLAST+: architecture and applications. *BMC Bioinformatics* **2009**, *10*, 421.
91. Tran-Nguyen, V.-K.; Jacquemard, C.; Rognan, D., LIT-PCBA: An Unbiased Data Set for Machine Learning and Virtual Screening. *Journal of Chemical Information and Modeling* **2020**, *60*, 4263-4273.
92. Dunbar, J. B., Jr.; Smith, R. D.; Yang, C. Y.; Ung, P. M.; Lexa, K. W.; Khazanov, N. A.; Stuckey, J. A.; Wang, S.; Carlson, H. A., CSAR benchmark exercise of 2010: selection of the protein-ligand complexes. *J Chem Inf Model* **2011**, *51*, 2036-46.
93. Aleksander, S. A.; Balhoff, J.; Carbon, S.; Cherry, J. M.; Drabkin, H. J.; Ebert, D.; Feuermann, M.; Gaudet, P.; Harris, N. L.; Hill, D. P.; Lee, R.; Mi, H.; Moxon, S.; Mungall, C. J.; Muruganugan, A.; Mushayahama, T.; Sternberg, P. W.; Thomas, P. D.; Van Auken, K.; Ramsey, J.; Siegele, D. A.; Chisholm, R. L.; Fey, P.; Aspromonte, M. C.; Nugnes, M. V.; Quaglia, F.; Tosatto, S.; Giglio, M.; Nadendla, S.; Antonazzo, G.; Attrill, H.; Dos Santos, G.; Marygold, S.; Strelets, V.; Tabone, C. J.; Thurmond, J.; Zhou, P.; Ahmed, S. H.; Asanithong, P.; Luna Buitrago, D.; Erdol, M. N.; Gage, M. C.; Ali Kadhum, M.; Li, K. Y. C.; Long, M.; Michalak, A.; Pesala, A.; Pritazhira, A.; Saverimuttu, S. C. C.; Su, R.; Thurlow, K. E.; Lovering, R. C.; Logie, C.; Oliferenko, S.; Blake, J.; Christie, K.; Corbani, L.; Dolan, M. E.; Drabkin, H. J.; Hill, D. P.; Ni, L.; Sitnikov, D.; Smith, C.; Cuzick, A.; Seager, J.; Cooper, L.; Elser, J.; Jaiswal, P.; Gupta, P.; Jaiswal, P.; Naithani, S.; Lera-Ramirez, M.; Rutherford, K.; Wood, V.; De Pons, J. L.; Dwinell, M. R.; Hayman, G. T.; Kaldunski, M. L.; Kwitek, A. E.; Laulederkind, S. J. F.; Tutaj, M. A.; VEDI, M.; Wang, S. J.; D'Eustachio, P.; Aimo, L.; Axelsen, K.; Bridge, A.; Hyka-Nouspikel, N.; Morgat, A.; Aleksander, S. A.; Cherry, J. M.; Engel, S. R.; Karra,

K.; Miyasato, S. R.; Nash, R. S.; Skrzypek, M. S.; Weng, S.; Wong, E. D.; Bakker, E.; Berardini, T. Z.; Reiser, L.; Auchincloss, A.; Axelsen, K.; Argoud-Puy, G.; Blatter, M. C.; Boutet, E.; Breuza, L.; Bridge, A.; Casals-Casas, C.; Coudert, E.; Estreicher, A.; Livia Famiglietti, M.; Feuermann, M.; Gos, A.; Gruaz-Gumowski, N.; Hulo, C.; Hyka-Nouspikel, N.; Jungo, F.; Le Mercier, P.; Lieberherr, D.; Masson, P.; Morgat, A.; Pedruzzi, I.; Pourcel, L.; Poux, S.; Rivoire, C.; Sundaram, S.; Bateman, A.; Bowler-Barnett, E.; Bye, A. J. H.; Denny, P.; Ignatchenko, A.; Ishtiaq, R.; Lock, A.; Lussi, Y.; Magrane, M.; Martin, M. J.; Orchard, S.; Raposo, P.; Speretta, E.; Tyagi, N.; Warner, K.; Zaru, R.; Diehl, A. D.; Lee, R.; Chan, J.; Diamantakis, S.; Raciti, D.; Zarowiecki, M.; Fisher, M.; James-Zorn, C.; Ponferrada, V.; Zorn, A.; Ramachandran, S.; Ruzicka, L.; Westerfield, M., The Gene Ontology knowledgebase in 2023. *Genetics* **2023**, *224*.

Table 1. Descriptions of meta-model feature groups

Feature Group ID	Description of features included	Feature list
<i>E</i>	Smina and Vinardo empirical (E) docking scores only	Smina score, Vinardo score
<i>EW</i>	E + molecular weight (MW)	Smina score, Vinardo score, MW
<i>ED1</i>	E + MW + Deep Learning (D) average scores from 6 BindingDB-pre-trained models provided in DeepPurpose v0.1.5	Smina score, Vinardo score, MW, CNN_CNN, Daylight_AAC, Morgan_AAC, Morgan_CNN, MPNN_CNN, Transformer_CNN
<i>ED2</i>	E + MW + D average scores from 6 models from DeepPurpose v0.0.1 trained <i>de novo</i> on BindingDB	Smina score, Vinardo score, MW, CNN_AAC, MPNN_CNN, CNN_CNN, Daylight_CNN, MPNN_AAC, MPNN_Transformer
<i>ED3</i>	E + MW + D average scores from 10 models from DeepPurpose 0.0.1 trained <i>de novo</i> on PDBbind	Smina score, Vinardo score, MW, CNN_AAC, MPNN_CNN, CNN_CNN, Daylight_CNN, MPNN_AAC, MPNN_Transformer, Daylight_AAC, Morgan_AAC, Morgan_CNN, Transformer_CNN
<i>ED1-F</i>	E + MW + D average of scores obtained from fine-tuning the <i>ED1</i> models, using PDBBind v2020 (the D scores are averaged for each model across 5 folds of cross-validation X 10 repetitions)	Smina score, Vinardo score, MW, CNN_CNN, Daylight_AAC, Morgan_AAC, Morgan_CNN, MPNN_CNN, Transformer_CNN
<i>ED2-F</i>	E + MW + D average of scores obtained from fine-tuning the <i>ED2</i> models, using PDBBind v2020 (the D scores are averaged for each model across 5 folds of cross-validation X 10 repetitions)	Smina score, Vinardo score, MW, CNN_AAC, MPNN_CNN, CNN_CNN, Daylight_CNN, MPNN_AAC, MPNN_Transformer
<i>ED1-F-P</i>	E + MW + D, where the reported scores are obtained by applying PCA to all scores from the 5 folds of cross-validation X 10 repetitions for the six models in <i>ED1-F</i>	Smina score, Vinardo score, MW, Up to 22 top PCs (determined for each machine learning method through hyperparameter optimization)
<i>ED2-F-P</i>	E + MW + D, where the reported scores are obtained by applying PCA to all scores from the 5 folds of cross-validation X 10 repetitions for the six models in <i>ED2-F</i>	Smina score, Vinardo score, MW, Up to 22 top PCs (determined for each machine learning method through hyperparameter optimization)
<i>ED3-P</i>	E + MW + D, where the reported scores are obtained by applying PCA to all scores from the 5 folds of cross-validation X 10 repetitions for the six models in <i>ED3</i>	Smina score, Vinardo score, MW, Up to 22 top PCs (determined for each machine learning method through hyperparameter optimization)
<i>ED-A-P</i>	E + MW + D, where the reported scores are obtained by applying PCA to all scores from the 5 folds of cross-validation X 10 repetitions for the models in <i>ED1-F</i> , <i>ED2-F</i> and <i>ED3</i>	Smina score, Vinardo score, MW, Up to 22 top PCs (determined for each machine learning method through hyperparameter optimization)

Table 2. Performances of DL models

Model	Training	Validation			
		PDBbind2020 Refined Set		CASF-2016 CoreSet	
		Pearson	MSE	Pearson	MSE
CNN_CNN	BindingDB pre-trained (D1)	0.424	18.734	0.358	25.116
Daylight_AAC		0.407	19.852	0.383	24.327
Morgan_AAC		0.465	17.859	0.343	25.274
Morgan_CNN		0.44	20.083	0.292	27.301
MPNN_CNN		0.47	21.167	0.333	27.685
Transformer_CNN		0.324	20.098	0.301	26.094
CNN-AAC	BindingDB de novo-trained (D2)	0.417	19.434	0.392	23.621
CNN-CNN		0.399	19.505	0.337	24.735
Daylight-CNN		0.382	21.756	0.461	24.559
MPNN-AAC		0.439	20.300	0.280	29.255
MPNN-CNN		0.417	22.031	0.286	30.418
MPNN-Transformer		0.237	26.710	0.297	27.936
CNN/RNN-CNN/RNN		0.235	24.322	0.261	28.996
MPNN-CNN/RNN		0.303	24.030	0.135	34.107
MPNN-PseudoAAC		0.351	20.376	0.333	26.823
MPNN-Quasi_seq		0.366	19.763	0.344	25.803
Transformer-Quasi_seq		0.002	23.456	-0.098	30.534
Transformer-Transformer		0.220	21.101	0.100	28.555
CNN-AAC	PDBbind2020 trained (D3)	0.929	2.913	0.76	10.581
CNN-CNN		0.91	3.671	0.733	11.624
Daylight_AAC		0.895	4.161	0.685	13.132
Daylight-CNN		0.875	4.933	0.599	15.767
Morgan_AAC		0.886	4.465	0.718	12.077
Morgan_CNN		0.926	3.078	0.644	14.375
MPNN-AAC		0.916	3.371	0.731	11.471
MPNN-CNN		0.897	4.121	0.727	11.76
MPNN-Transformer		0.922	3.161	0.737	11.29
Transformer_CNN		0.824	6.681	0.553	17.155
CNN_CNN	BindingDB pre-trained & PDBbind fine-tuned (D1F)	0.844	5.846	0.691	12.891
Daylight_AAC		0.861	6.615	0.628	16.728
Morgan_AAC		0.874	5.154	0.677	13.98
Morgan_CNN		0.887	4.398	0.637	14.739
MPNN_CNN		0.873	5.04	0.634	15.042
Transformer_CNN		0.751	8.84	0.489	19.17
PC1		NA	NA	0.715	NA
CNN-AAC	BindingDB de novo-trained & PDBbind fine-tuned (D2F)	0.841	6.618	0.627	16.344
CNN-CNN		0.872	5.907	0.654	15.773
Daylight-CNN		0.829	6.5	0.613	15.694
MPNN-AAC		0.894	4.162	0.663	13.882
MPNN-CNN		0.895	4.113	0.654	14.2
MPNN-Transformer		0.876	5.465	0.637	15.822
PC1		NA	NA	0.749	NA

Table 3. Meta-model performances by XGboost

Feature groups	Pearson					MSE				
	Consensus		RelExpt			Consensus		RelExpt		
	101	3	101	100	3	101	3	101	100	3
E	0.527	0.527	0.547	0.536	0.628	18.192	16.756	17.761	17.459	12.529
EW	0.587	0.568	0.586	0.605	0.639	16.997	15.907	16.842	15.804	12.226
ED1	0.600	0.598	0.620	0.636	0.671	16.000	14.765	15.504	14.914	11.235
ED2	0.639	0.626	0.645	0.657	0.702	15.030	14.125	14.753	14.249	10.426
ED3	0.753	0.743	0.750	0.758	0.717	10.587	10.163	10.728	10.340	9.717
ED1-F	0.722	0.694	0.722	0.714	0.703	11.730	11.779	11.742	11.902	10.175
ED2-F	0.750	0.739	0.750	0.752	0.704	10.748	10.339	10.757	10.579	10.139
ED1-F-P	0.747	0.731	0.755	0.749	0.735	10.951	10.650	10.664	10.763	9.149
ED2-F-P	0.768	0.750	0.768	0.770	0.732	10.164	9.967	10.198	9.973	9.267
ED3-P	0.777	0.764	0.778	0.773	0.769	9.920	9.602	9.879	10.013	8.202
ED-A-P	0.763	0.759	0.764	0.776	0.765	10.420	9.804	10.437	9.951	8.368

Table 4. Performance comparisons of a virtual screening benchmark

Performance metric	RMSE			PCC		
	O60341	O15151	POC6U8	O60341	O15151	POC6U8
Number of ligands	20	8	7	20	8	7
E (docking)	5.04	10.45	5.82	-0.18	-0.07	0.57
D (deep learning)	2.34	2.20	1.01	0.72	0.59	0.94
Meta-models	2.34	1.44	2.12	0.64	0.95	0.92
HAC-Net	5.13	7.16	5.58	0.33	0.23	0.80
SG-CNN (FAST)*	2.10	1.37	1.80	-0.38	0.25	-0.59
KDeep	4.99	3.68	6.01	-0.17	0.60	0.14

N.B. The best performance value for each target protein is in bold italic, while performance values for our models are in bold. PCC = Pearson correlation coefficient. *Pre-trained on PDBbind v2016 GeneralSet.

Table 5. Enrichment of active ligands in the top predicted ligands for LIT-PCBA virtual screening

Target	DL models			Meta-models			SMINA			Vinardo		
	Top5	Actives	Fraction	Top5	Actives	Fraction	Top5	Actives	Fraction	Top5	Actives	Fraction
ADRB2	2		0.4	2		0.4	2		0.4	3		0.6
ALDH1	2		0.4	4		0.8	3		0.6	3		0.6
ESR1_ago	4		0.8	4		0.8	3		0.6	4		0.8
ESR1_ant	4		0.8	4		0.8	3		0.6	3		0.6
FEN1	4		0.8	4		0.8	2		0.4	2		0.4
GBA	4		0.8	4		0.8	4		0.8	4		0.8
IDH1	4		0.8	4		0.8	2		0.4	2		0.4
KAT2A	3		0.6	3		0.6	3		0.6	2		0.4
MAPK1	3		0.6	3		0.6	4		0.8	3		0.6
MTORC1	3		0.6	2		0.4	3		0.6	3		0.6
OPRK1	4		0.8	3		0.6	4		0.8	3		0.6
PKM2	4		0.8	4		0.8	3		0.6	3		0.6
PPARG	1		0.2	1		0.2	3		0.6	3		0.6
TP53	1		0.2	1		0.2	4		0.8	3		0.6
VDR	3		0.6	3		0.6	2		0.4	3		0.6

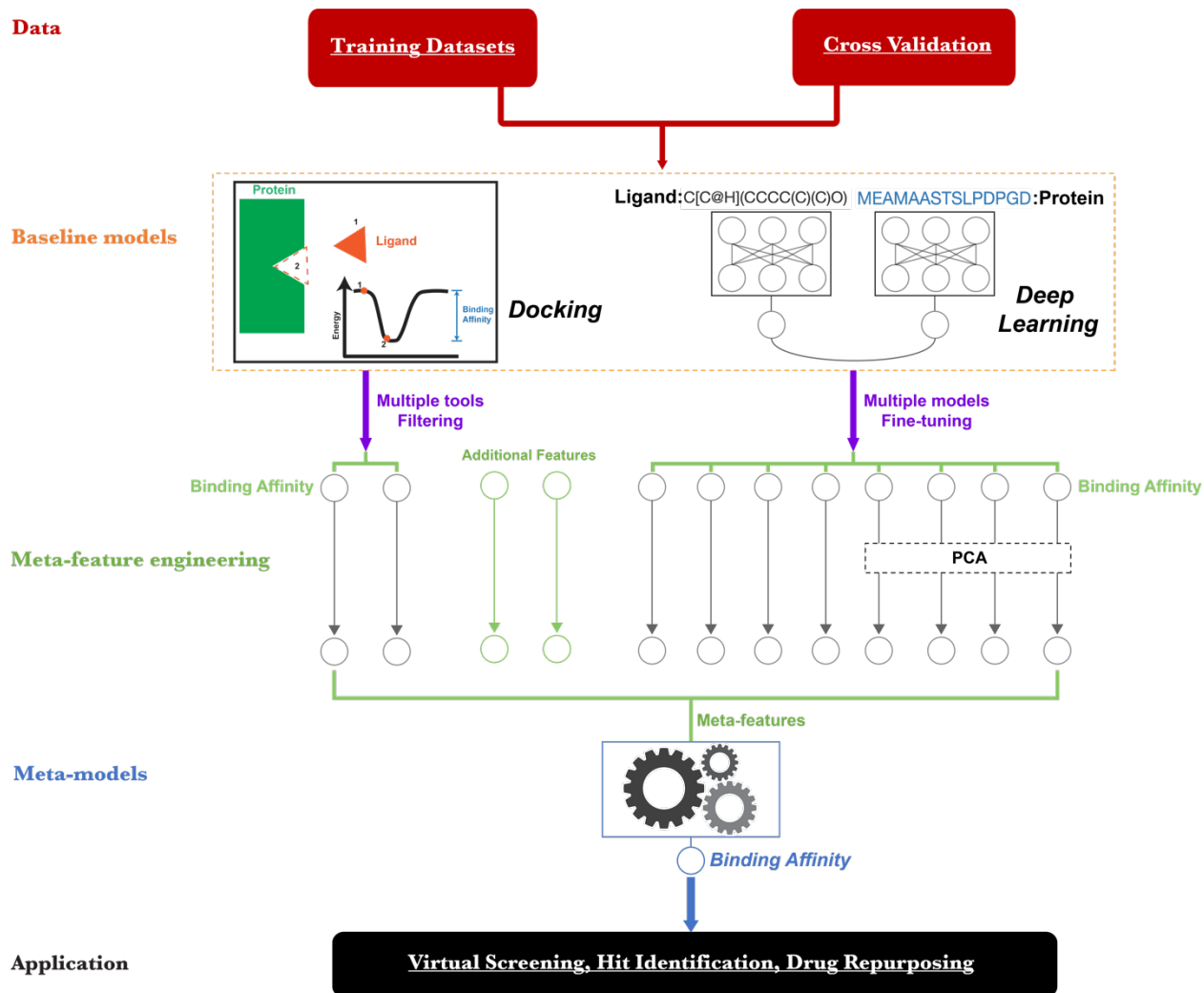


Figure 1. Overview of our workflow. The inputs are training datasets (BindingDB and PDBbind) and a cross-validation strategy. The baseline models consist of docking tools (SMINA and Vinardo) and deep-learning (DL) models (from the DeepPurpose library). The DL models were either pre-trained or *de novo* trained, while the docking tools were pre-trained. The output ligand poses of the docking tools are filtered by structural comparisons with the experimental docked poses, or by comparisons between the poses predicted by the two docking tools. The BindingDB-trained DL models are fine-tuned on the PDBbind dataset, and their prediction scores are further transformed through principal component analysis (PCA). Additional features, such as molecular weight, can be added, before various combinations of all these meta-features (filtered or unfiltered docking scores, fine-tuned and/or PCA-transformed DL scores) are fed into several machine-learning meta-models for final training on the PDBbind dataset. The meta-models include linear regression, LASSO, ElasticNet, and XGBoost.

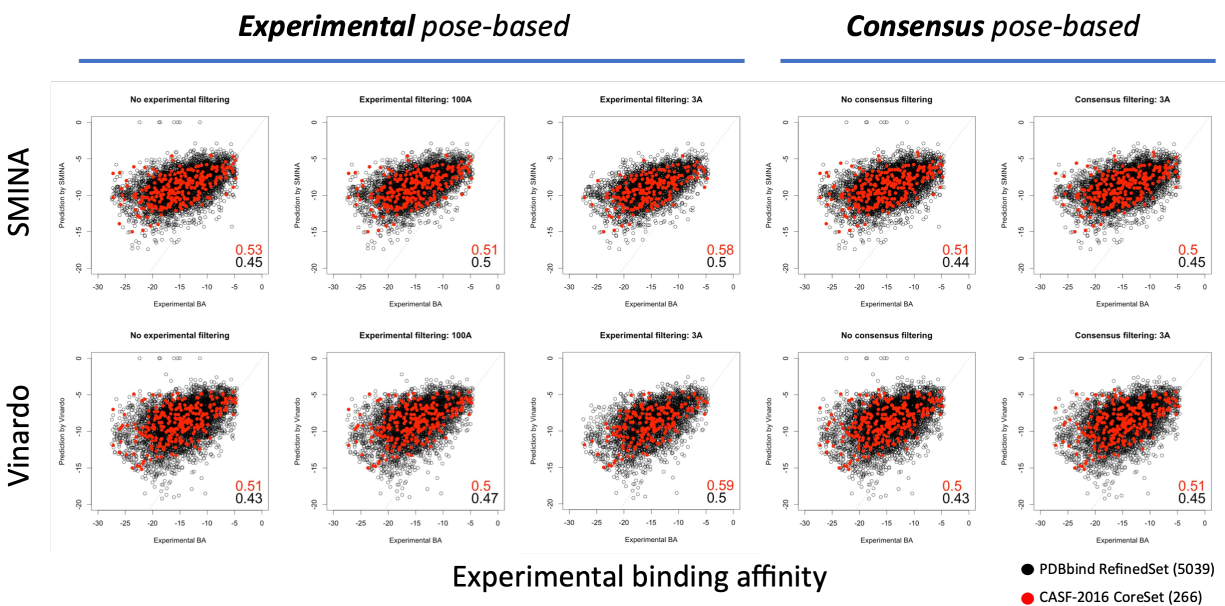


Figure 2. Performances of empirical scoring functions and consensus filtering. The outputs of the docking tools, SMINA and Vinardo, are shown with the binding affinities for the RefinedSet\CoreSet in black and those for the CoreSet in red. The columns indicate the different choices of filtering approaches and pose-based RMSD thresholds. Pearson’s correlation values for the two different sets of predictions are shown in each panel in their respective colors.

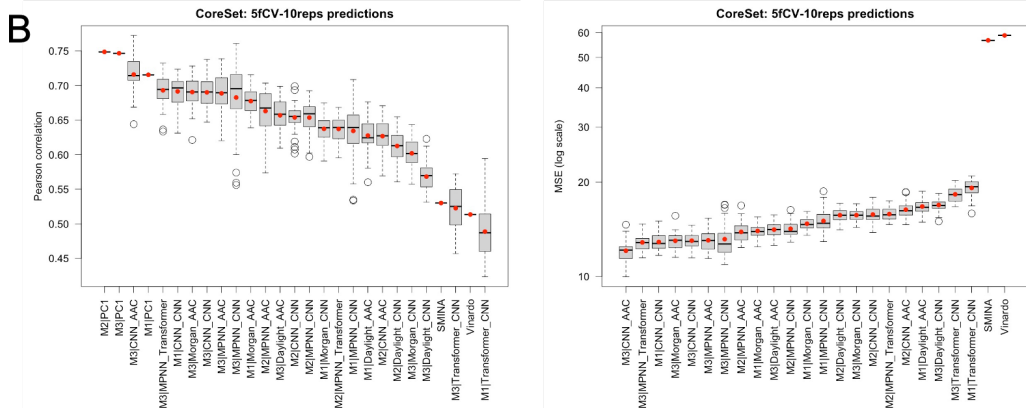
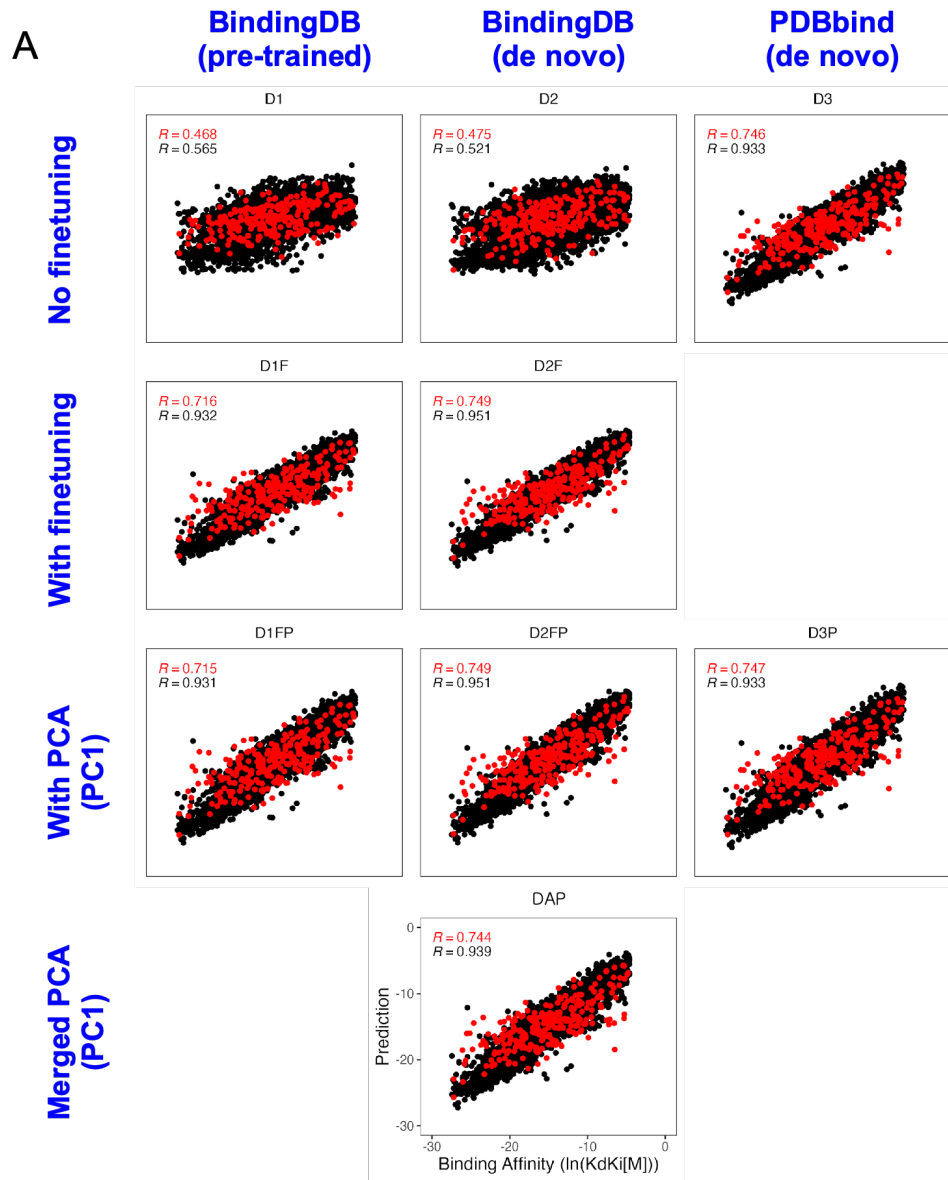


Figure 3. Performances of deep learning models. (A) Scatter plots of experimental binding affinities (x axis) and model predictions (y axis) for the full 5,305 complexes in the PDBbind RefinedSet (266 complexes in the CoreSet benchmark). Each plot shows predictions by the average of the best models or PC1 in terms of Pearson correlation coefficients for the CoreSet in each training strategy. (B) Box-whisker plots of Pearson correlation coefficients (left panel) and mean squared errors (MSE; right panel) for the CoreSet by a total of 22 PDBbind-finetuned (M1 and M2) and PDBbind-trained (M3) models and PC1 models of M1, M2, and M3 along with SMINA and Vinardo models. Predictions of the 22 models are mean values from 10 repeated 5-fold CVs. M1, M2, and M3 correspond to D1F, D2F, and D3 in (A).

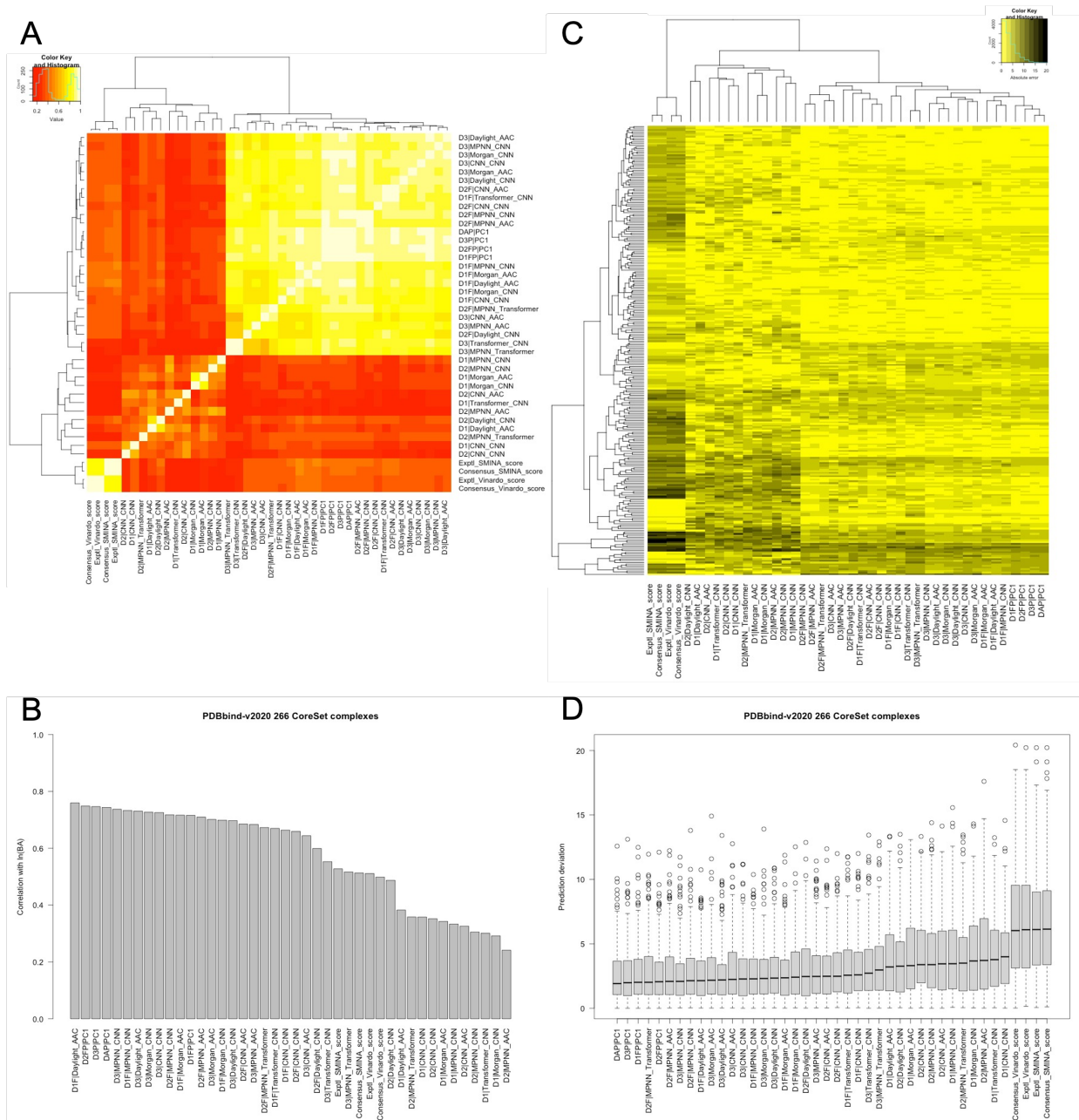


Figure 4. Model comparison of CoreSet predictions. (A) Heatmap of Pearson correlations between all pairs of CoreSet predictions by the 42 models from the docking and deep learning tools. The dendrograms are results of hierarchical clustering with Euclidean distance and the complete linkage method. (B) Bar plot of Pearson correlations between the experimental binding affinity and predictions by the 42 models for the CoreSet complexes. The models are ordered by the correlation values. (C) Heatmap of absolute errors or deviations between the experimental binding affinity and predictions by the 42 models (columns) for each of the CoreSet complexes (rows). The dendrograms are as in (A). (D) Box-whisker plot of the data used in (B). The models are ordered by the median values.

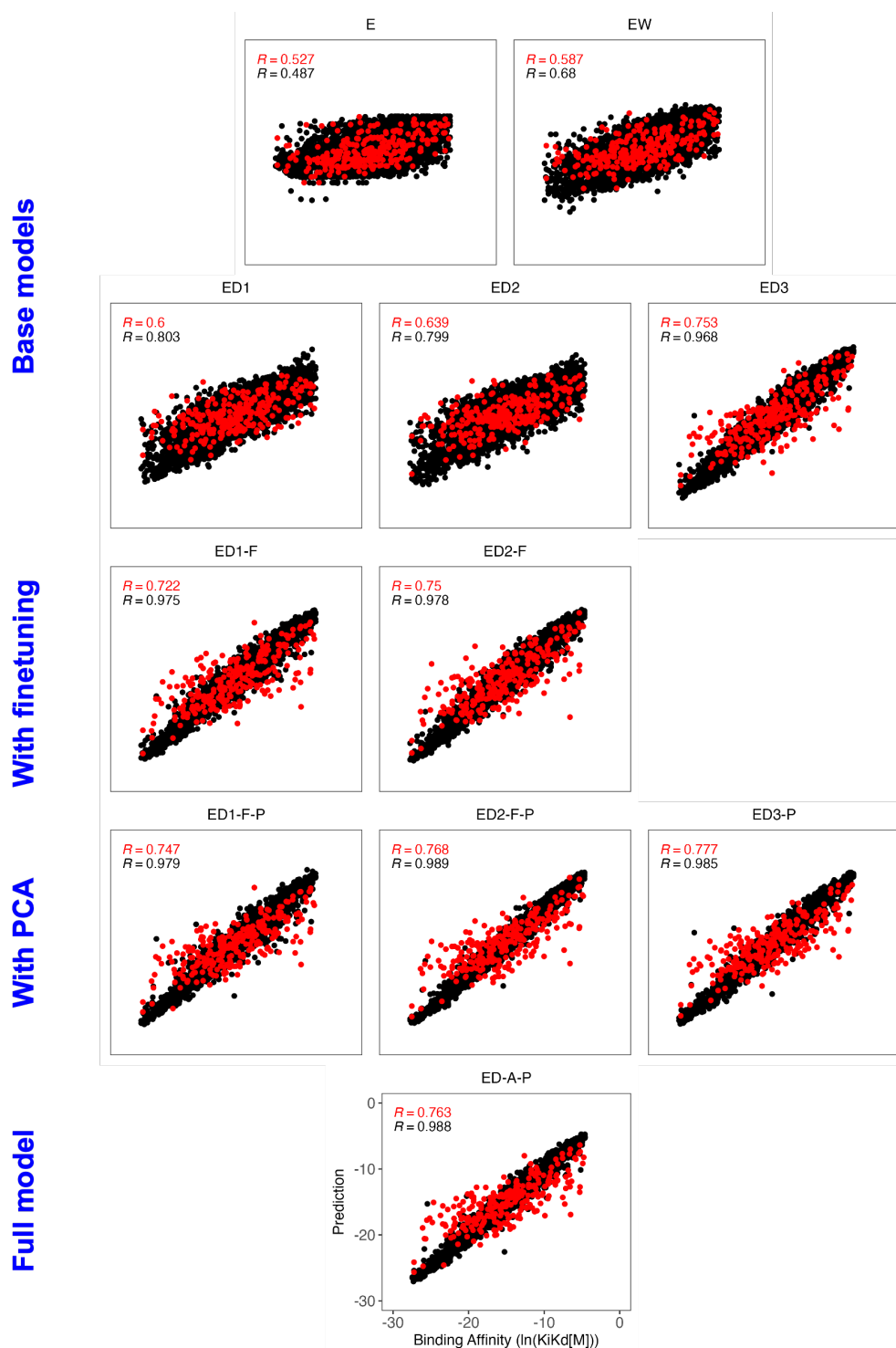


Figure 5. Performances of meta-models. Predictions by XGBoost for the unfiltered training set are shown. The first row represents the meta-models constructed entirely based on the docking methods,

SMINA and Vinardo. The first panel shows results for the two scores alone (E), while the second panel shows the results also including the molecular weight parameter (EW). The remaining rows show results for meta-models that include DL scores. The second, third and fourth rows represent successive processing of the deep learning model scores, with the second row showing the average scores (ED1, ED2, ED3), the third row (if a panel is present) showing the average after fine-tuning (F) using the RefinedSet\CoreSet (ED1-F, ED2-F), and the fourth row showing the scores using the optimal number of PCs from a PCA (P) on the previous level (either fine-tuned or not) (ED1-F-P, ED2-F-P, ED3-P). The columns of the second, third and fourth rows show the three different base training sets used for the DL scores, where the leftmost column is based on the pre-trained models on BindingDB (ED1 series), the central column is based on the de novo-trained models on BindingDB (ED2 series) and the rightmost column is based on the de novo-trained models on PDBbind (ED3 series). The single panel in the last fifth row shows the results for the meta-model ED-A-P, which is based on a PCA on all the training scores from ED1-F, ED2-F, and ED3.

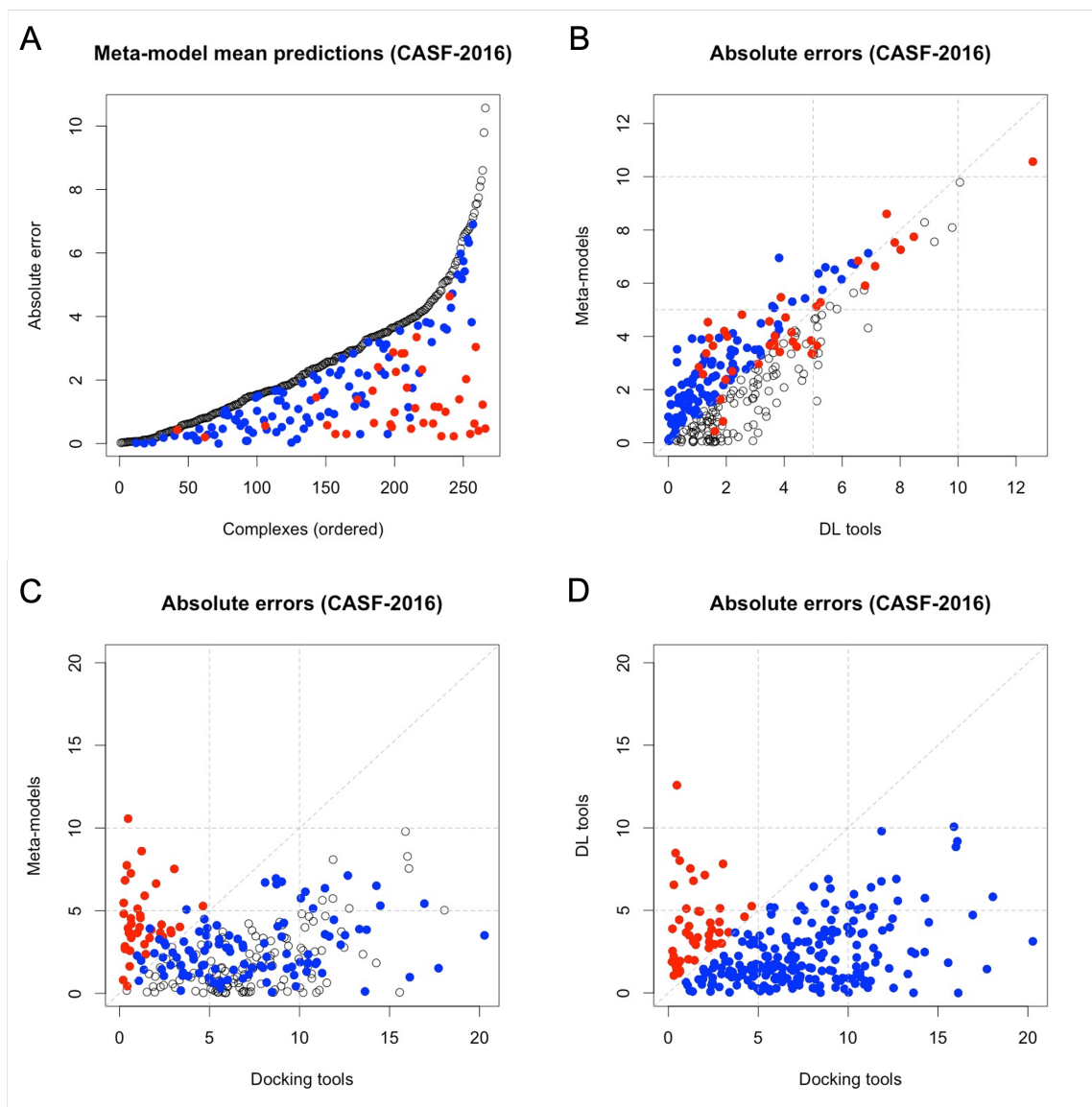


Figure 6. Prediction synergy and complementarity of docking and DL tools by meta-modeling. (A) Absolute errors (AEs) of the mean predictions for the CASF-2016 benchmark set (266 complexes) by the 4 meta-models with ED-A-P (open circles; ordered by AEs). The blue circles correspond to 104 complexes (39.1%) whose predictions by the DL tools (DAP|PC1 in **Fig. 4D**) are better than the mean predictions by the 4 meta-models or the 4 docking tools (i.e., lower AEs). The red circles correspond to 39 complexes (14.7%) whose mean predictions by the 4 docking tools are better than those by the meta-models or the DAP|PC1. (B-D) Scatter plots of AEs of the (mean) predictions for the CASF-2016 benchmark set by the DAP|PC1 vs. the 4 meta-models (B), by the 4 docking tools vs. the 4 meta-models (C), and by the 4 docking tools vs. the DAP|PC1 (D). The blue and red dots in (B) and (C) correspond to those in (A). In (D), the 48 complexes (18.0%) in red indicate better predictions (i.e., lower AEs) by the docking tools on average, whereas the remaining 218 complexes (82.0%) in blue indicate better predictions by the DAP|PC1.

Supporting Information

Improved Prediction Of Ligand-Protein Binding Affinities By Meta-Modeling

Ho-Joon Lee^{1,2,*#}, Prashant S. Emani^{3,*#} and Mark B. Gerstein^{3,4,5,6,7#}

¹Dept. of Genetics and ²Yale Center for Genome Analysis, Yale University, New Haven, CT 06510, USA

³Dept. of Molecular Biophysics & Biochemistry, Yale University, New Haven, CT 06520, USA ⁴Program in Computational Biology & Bioinformatics, ⁵Dept. of Computer Science, ⁶Dept. of Statistics & Data Science, and ⁷Dept. of Biomedical Informatics & Data Science, Yale University, New Haven, CT 06520, USA

* Equal contributions

Correspondence: HL, ho-joon.lee@yale.edu; PSE, prashant.emani@yale.edu; MBG, pi@gersteinlab.org

Supplementary Methods

Docking Methods

We have constructed custom Python wrapper scripts to implement the entire pipeline, with slight variations depending on the dataset considered. We describe the essential aspects of running a docking simulation in the following.

1. *Selection of the receptor structure file:* All data files for each complex in the PDBbind dataset¹ are contained in separate subfolders. We utilized the protein PDB file for the remaining processing steps.
2. *Preparation of the receptor structure:* The receptor structure is read in as a PDB file and preprocessed in PyMol (<https://pymol.org>). We used the *pymol* class and associated functions within our pipeline script. The preprocessing consists of the removal of *all* solvent and heteroatoms in the molecules. The resulting PDB file is then converted into the requisite PDBQT format using OpenBabel (<http://openbabel.org>). We used the *obabel* flags ‘-e = continue after errors’, ‘-p = add hydrogens appropriate for the pH’, and ‘--partialcharge gasteiger’ to calculate Gasteiger partial charges. The pH was set at 7.0. We included the PDBQT-specific flags ‘r = output as a rigid molecular’ and ‘p = Preserve atom indices from input file’. The implementation of this is written as:

```
obabel -ipdb <Input PDB file> -opdbqt -O <Output PDBQT file> -p 7.0 -e -xrp --partialcharge gasteiger
```


(Note the ‘-x’ flag is set to enable the output-specific flags, which are PDBQT-specific in our case.)
3. *Ligand files:* Given the use of 3D SDF files for all analyses, the ligand files did not need further processing. The appropriate ligand SDF files were invoked in the docking command (see below), including the complex-specific ligand files in the PDBbind dataset (the ligand SDF files are included in the subfolders for each complex).
4. *Creation of the configuration file:* The configuration file serves to provide a set of commands to the *smina* package² (as well as the original AutoDock Vina tool³). The file contains the receptor PDBQT file, the ligand SDF file, the center coordinates of the search box in the receptor structure file coordinate system, and the dimensions of the search box. The calculation of the center coordinates varies depending on the datasets under consideration. For the PDBbind dataset, we used the center of mass of each ligand SDF file as the center of the search box, employing PyMol’s *centerofmass* function to do so. The search box was set to have dimensions of 40 Angstroms in the x, y and z directions.
5. *Running the docking software:* Using the configuration file and the ligand file name, we ran the program *smina* using both the default (hereafter termed “SMINA”) and “Vinardo” scoring functions. We used an *exhaustiveness* parameter of 32 and used the default output of the top 9 poses (ranked from 0 to 8 from lowest to highest binding energy). The program call was:

```
smina --config <config_file> --out <Output Complex PDBQT file> --log <Log file containing binding affinities> --exhaustiveness 32
```

Implementation of RMSD filters

For the RMSD filters, we calculate $RMSD_{ab}$ in two ways, depending on the choice of docking poses:

- a. **Experimental pose-RMSD filtering:** The deviation is calculated for a ligand pose predicted by a docking method relative to the experimental structure of the ligand. Ligands were assigned an RMSD of 100 Angstroms if either of the docking tools failed to generate a docked structure, or if the bond

reordering process (see **Supplementary Methods**) failed. In those cases, we automatically selected the lowest energy pose out of the 9 outputs by the docking tools. After reordering, the symmetric RMSD was calculated, and we filtered the poses for each complex by an RMSD cutoff of 3 Angstroms. Among those poses that satisfied the cutoff we chose the lowest energy structure. If no poses met the cutoff, then we selected the lowest energy pose with the RMSD set to 100 Angstroms. In this way, we had two tiers of poses from all the complexes: a set of docked poses with RMSD relative to the experimental poses < 3 Angstroms (and which may not have been the lowest energy pose among the 9 docking poses); and another set where the lowest energy pose was selected with an arbitrarily set RMSD of 100 Angstroms (for downstream filtering purposes).

- b. **Consensus pose-RMSD filtering:** This is where the deviation is calculated between the docking poses for the same ligand-target pair as predicted by two different docking methods. In our analyses, these correspond to the poses from the SMINA and Vinardo scoring functions. For the Vinardo and SMINA pose comparisons, we had $9 \times 9 = 81$ pairs of docked poses to filter through for the final assignment of RMSD. In the case of docked pose comparisons, there was no need for bond reordering, as *smina* generated poses with the same ordering convention using both scoring functions. The RMSD was calculated for all pairs of docking poses for each complex and the [SMINA, Vinardo] pair with an RMSD less than 3 Angstroms and with the lowest rank sum (SMINA rank + Vinardo rank) was chosen in the final scoring. If multiple pairs had the same rank sum, the pair with the lowest RMSD was selected. If a complex had no pairs with an RMSD less than 3 Angstroms, then the lowest energy poses from both methods were selected and assigned a pairwise RMSD of 100 Angstroms for downstream filtering. As a result of this assignment process, all structures with an RMSD < 100 Angstroms will necessarily have an RMSD < 3 Angstroms. We thus only need to consider one of the two cases in the results.

Note on the coding of *Experimental pose-RMSD filtering*: The experimental structures are available, in our analyses, in the PDBbind dataset in SDF and MOL2 formats. The calculation of this RMSD in Pymol’s Python API (<http://www.pymol.org/pymol>) involved first reordering the bonds in the docking pose using either the experimental structure or the SMILES string as a “template”, as the atoms are not consistently designated between the *smina* predicted poses and the experimental structures. This was followed by the calculation of the RMSD between the experimental and reordered predicted pose. The bond reordering process was carried out using the experimental mol2 file (for the PDBbind structures), using functions in the Python package RDKit (www.rdkit.org/).

Meta-models

We used linear regression, ElasticNet, and LASSO algorithms for linear meta-models and the XGBoost algorithm for a non-linear meta-model implemented in *scikit-learn* in Python⁴. The steps in the preprocessing of the PDBbind dataset were as follows:

1. The predicted binding affinity matrices from the docking and deep learning tools were merged based on the PDB IDs.
2. We separately incorporated the RMSD values for the complexes (either based on ‘Experimental’ or ‘Consensus’ quantifications) into the merged binding affinity matrix.
3. Those structures in the non-core-set not satisfying the RMSD cutoffs were removed from further analysis. We did not apply the RMSD filters to the core set.
4. We also calculated the molecular weight of the ligands and allowed for the possibility of incorporating these values into the binding affinity matrix (this is enabled by a separate flag in the code, which either includes or excludes the molecular weight).

5. All structures in the core set of the PDBbind cohort are set aside for the test scoring. The remainder of the binding affinity matrix is carried forward for the analysis.
6. The binding affinity matrix for the training set (the non-core-set portion of the PDBbind refined set) was separated into feature (X) and target value (y) numpy arrays.

These trainsets were input to the meta-models. The parameters used in each of the models are:

- A. **LASSO model:** We iterated *scikit-learn*'s LassoCV approach 100 times with shuffled data, using 5-fold cross-validation each time. The best model chosen was the one with the minimum 'dual_gap_' score.
- B. **ElasticNet model:** We iterated *scikit-learn*'s ElasticNetCV approach 10 times for each L1_ratio in the list [.1, .5, .7, .9, .95, .99, 1] (the L1_ratio parameter is the balance between the L1 and L2 penalties in the ElasticNet method). Each iteration used shuffled data and 5-fold cross-validation. The best model chosen overall was the one with the minimum 'dual_gap_' score.
- C. **Linear Regression model:** We ran linear regression with no additional parameters or regularization penalties.
- D. **XGBoost model:** We used the *xgboost.XGBRegressor* model class with a "squared-error" objective (https://xgboost.readthedocs.io/en/release_0.72/python). This model was then used in *scikit-learn*'s RandomizedSearchCV method to run 100 iterations with 5-fold cross-validation, comprehensively exploring several parameters within reasonable ranges: "colsample_bytree" uniformly in the range [0.8, 0.2]; "gamma" uniformly in the range [0, 0.5]; "learning_rate" uniformly in the range [0.02, 0.3]; "max_depth" randomly from the set of integers in the range [2, 6]; "n_estimators" randomly from the set of integers in the range [100, 150]; "subsample" uniformly in the range [0.7, 0.3]. The maximum 'mean_test_score' was used to select the best model.

SwissADME Analysis

To understand the contributions of ligand properties to performance of all the models, we used the web tool *SwissADME*⁵ to extract the properties of the PDBbind CoreSet ligands from their SMILES strings. We first converted the ligand SMILES strings to canonical SMILES format using OpenBabel (<http://openbabel.org>). We then submitted the canonical SMILES strings to SwissADME's web interface. This yielded a set of 46 properties for 263 ligands in the CoreSet. We subsequently sought to measure the correlation between the deviation of the predicted scores from the experimental values with the numerical features, to identify those ligand features that might contribute to reduced performance of the model.

We also investigated the SwissADME features that might be associated with better or worse performance for subsets of complexes by the different groups of tools (docking, DL, and meta-models). We checked for duplicate SMILES strings for the ligands and found none, thus requiring no further filtration. Using two-sided Wilcoxon and t-tests, we compared the distributions for all the numeric SwissADME features.

UniProt Analysis

To identify protein features that might be associated with better or worse performance of specific tools, we extracted the relevant subsets of PDBbind CoreSet PDB IDs from our analyses and fed them into the "Retrieve/ID mapping" tool of the UniProt database (www.uniprot.org/id-mapping)⁶. The corresponding UniProt IDs and the following features were downloaded in a .tsv file: 'From', 'Entry', 'Reviewed', 'Entry

Name', 'Protein names', 'Gene Names', 'Organism', 'Length', 'Active site', 'Binding site', 'Function [CC]', 'Catalytic activity', 'Annotation', 'Gene Ontology (biological process)', 'Helix', 'Turn', 'Beta strand', 'Coiled coil', 'Compositional bias', 'Domain [CC]', 'Domain [FT]', 'Motif', 'Protein families', 'Region', 'Repeat', 'Zinc finger', 'Pathway', 'Gene Ontology (molecular function)', 'Post-translational modification'. We first filtered out all UniProt entries that were not labeled "reviewed". Next, we manually checked repeats, where the same PDB ID mapped to multiple UniProt IDs, by looking up the PDB IDs on the RCSB PDB website (www.rcsb.org/). We checked both the "Gene Names" and "Species" and removed all UniProt entries that did not match the PDB entry. In all cases, this left only a single PDB ID-UniProt ID mapping for each PDB ID. Additionally, to run the tests of over- or under-representation, we also deduplicated the UniProt IDs. That is, we removed all cases of proteins that were represented more than once, as the CoreSet has a large number of proteins that recur in the dataset. This led to a significant reduction in the number of proteins tested for UniProt feature prioritization from 266 to 60. Fisher's exact test was run when comparing the number of occurrences of a feature in the subset versus the whole. The features tested are: the number of times a given UniProt term was annotated at all; the occurrence of Gene Ontology⁷ terms, both the "Biological Process" and "Molecular Function" categories; and protein Domain and Pathway annotations.

LIT-PCBA Virtual Screening

For the LIT-PCBA virtual screening exercise, we utilized balanced sets of 10 active and 10 inactive ligands randomly drawn from the combined training and validation cohorts of the LIT_PCBA database⁸. To run the docking tools on the datasets, we generated three-dimensional SDF structures for each of the ligands from their SMILES strings using the following command:

```
obabel -:'<SMILES string>' --gen2d -omol | obabel -imol --minimize --noh -omol | obabel -imol -h -e --gen3d -osdf -O '<output SDF file>'
```

We also utilized the LIT-PCBA-provided PDB structures for the protein-ligand complex to configure the docking, by removing solvent molecules and other heteroatoms from the mol2 structure of the protein and then using the center-of-mass coordinates of the corresponding docked ligand in the PDB complex to define the docking search box. This facilitates a search for poses within the same binding pocket as the template complex provided by LIT-PCBA.

Supplementary References

1. Liu, Z.; Su, M.; Han, L.; Liu, J.; Yang, Q.; Li, Y.; Wang, R., Forging the Basis for Developing Protein–Ligand Interaction Scoring Functions. *Accounts of Chemical Research* 2017, 50 (2), 302-309.
2. Koes, D. R.; Baumgartner, M. P.; Camacho, C. J., Lessons learned in empirical scoring with smina from the CSAR 2011 benchmarking exercise. *J Chem Inf Model* 2013, 53 (8), 1893-904.
3. Trott, O.; Olson, A. J., AutoDock Vina: improving the speed and accuracy of docking with a new scoring function, efficient optimization, and multithreading. *J Comput Chem* 2010, 31 (2), 455-61.
4. Pedregosa, F.; Varoquaux, G.; Gramfort, A.; Michel, V.; Thirion, B.; Grisel, O.; Blondel, M.; Prettenhofer, P.; Weiss, R.; Dubourg, V.; Vanderplas, J.; Passos, A.; Cournapeau, D.; Brucher, M.; Perrot, M.; Duchesnay, É., Scikit-learn: Machine Learning in Python. *J. Mach. Learn. Res.* 2011, 12 (null), 2825–2830.
5. Daina, A.; Michielin, O.; Zoete, V., SwissADME: a free web tool to evaluate pharmacokinetics, drug-likeness and medicinal chemistry friendliness of small molecules. *Scientific reports* 2017, 7 (1), 42717.
6. The UniProt Consortium, UniProt: the Universal Protein Knowledgebase in 2023. *Nucleic acids research* 2023, 51 (D1), D523-d531.
7. Aleksander, S. A.; Balhoff, J.; Carbon, S.; Cherry, J. M.; Drabkin, H. J.; Ebert, D.; Feuermann, M.; Gaudet, P.; Harris, N. L.; Hill, D. P.; Lee, R.; Mi, H.; Moxon, S.; Mungall, C. J.; Muruganugan, A.; Mushayahama, T.; Sternberg, P. W.; Thomas, P. D.; Van Auken, K.; Ramsey, J.; Siegele, D. A.; Chisholm, R. L.; Fey, P.; Aspromonte, M. C.; Nugnes, M. V.; Quaglia, F.; Tosatto, S.; Giglio, M.; Nadendla, S.; Antonazzo, G.; Attrill, H.; Dos Santos, G.; Marygold, S.; Strelets, V.; Tabone, C. J.; Thurmond, J.; Zhou, P.; Ahmed, S. H.; Asanitthong, P.; Luna Buitrago, D.; Erdol, M. N.; Gage, M. C.; Ali Kadhum, M.; Li, K. Y. C.; Long, M.; Michalak, A.; Pesala, A.; Pritazahra, A.; Saverimuttu, S. C. C.; Su, R.; Thurlow, K. E.; Lovering, R. C.; Logie, C.; Oliferenko, S.; Blake, J.; Christie, K.; Corbani, L.; Dolan, M. E.; Drabkin, H. J.; Hill, D. P.; Ni, L.; Sitnikov, D.; Smith, C.; Cuzick, A.; Seager, J.; Cooper, L.; Elser, J.; Jaiswal, P.; Gupta, P.; Jaiswal, P.; Naithani, S.; Lera-Ramirez, M.; Rutherford, K.; Wood, V.; De Pons, J. L.; Dwinell, M. R.; Hayman, G. T.; Kaldunski, M. L.; Kwitek, A. E.; Laulederkind, S. J. F.; Tutaj, M. A.; Vedi, M.; Wang, S. J.; D'Eustachio, P.; Aimo, L.; Axelsen, K.; Bridge, A.; Hyka-Nouspikel, N.; Morgat, A.; Aleksander, S. A.; Cherry, J. M.; Engel, S. R.; Karra, K.; Miyasato, S. R.; Nash, R. S.; Skrzypek, M. S.; Weng, S.; Wong, E. D.; Bakker, E.; Berardini, T. Z.; Reiser, L.; Auchincloss, A.; Axelsen, K.; Argoud-Puy, G.; Blatter, M. C.; Boutet, E.; Breuza, L.; Bridge, A.; Casals-Casas, C.; Coudert, E.; Estreicher, A.; Livia Famiglietti, M.; Feuermann, M.; Gos, A.; Gruaz-Gumowski, N.; Hulo, C.; Hyka-Nouspikel, N.; Jungo, F.; Le Mercier, P.; Lieberherr, D.; Masson, P.; Morgat, A.; Pedruzzi, I.; Pourcel, L.; Poux, S.; Rivoire, C.; Sundaram, S.; Bateman, A.; Bowler-Barnett, E.; Bye, A. J. H.; Denny, P.; Ignatchenko, A.; Ishtiaq, R.; Lock, A.; Lussi, Y.; Magrane, M.; Martin, M. J.; Orchard, S.; Raposo, P.; Speretta, E.; Tyagi, N.; Warner, K.; Zaru, R.; Diehl, A. D.; Lee, R.; Chan, J.; Diamantakis, S.; Raciti, D.; Zarowiecki, M.; Fisher, M.; James-Zorn, C.; Ponferrada, V.; Zorn, A.; Ramachandran, S.; Ruzicka, L.; Westerfield, M., The Gene Ontology knowledgebase in 2023. *Genetics* 2023, 224 (1).
8. Tran-Nguyen, V.-K.; Jacquemard, C.; Rognan, D., LIT-PCBA: An Unbiased Data Set for Machine Learning and Virtual Screening. *Journal of Chemical Information and Modeling* 2020, 60 (9), 4263-4273.

Supplementary Figures

Figure S1. Overview of our workflow with an example meta-model of ED1-F-P.

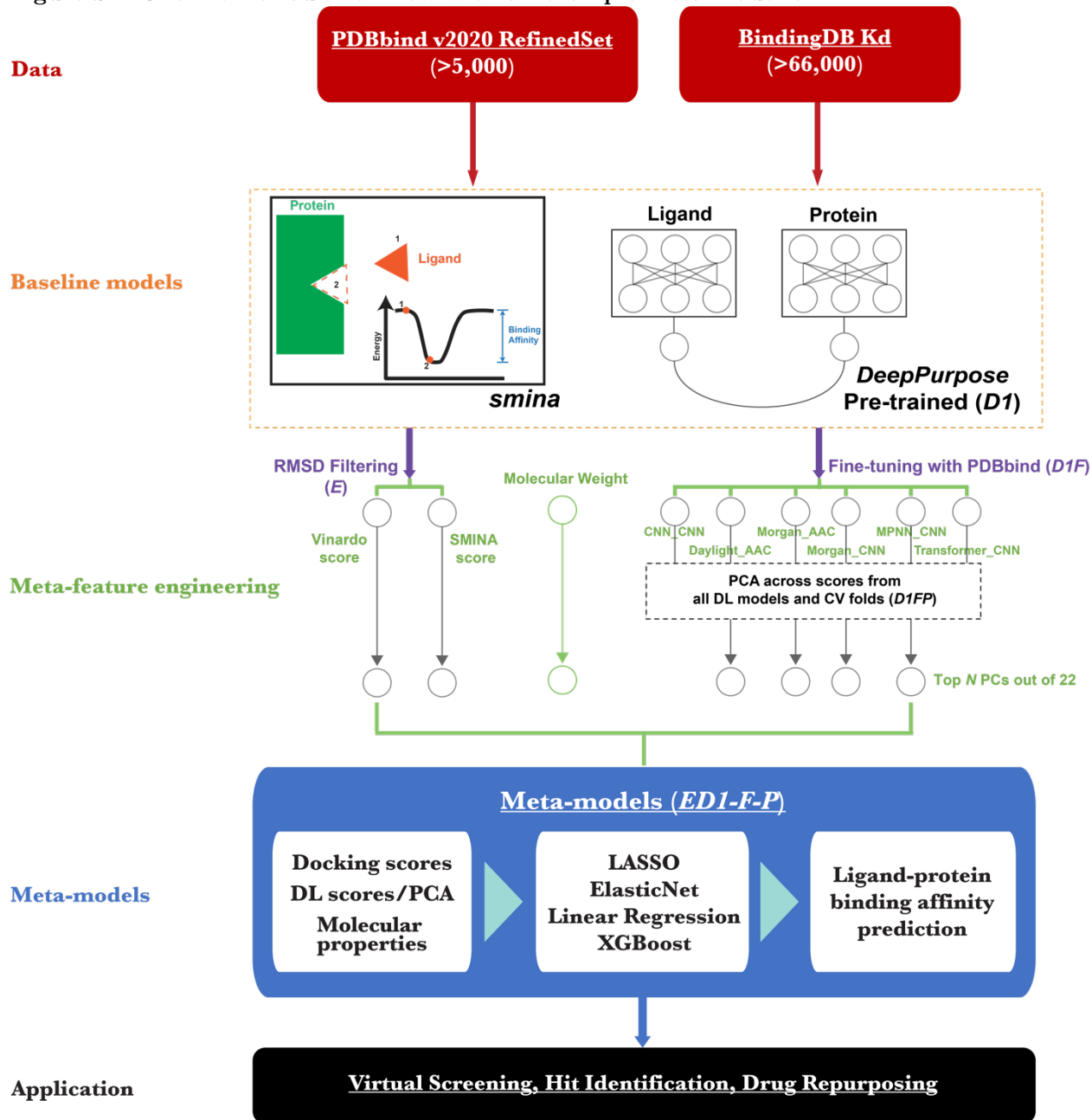


Figure S2. Ligand pose-based filtering for the docking tools. (A) RMSD distributions for the experimental pose-based and consensus pose-based filtering strategies (266 CASF-2016 complexes in red) (B) Monte Carlo simulations of prediction correlations for the CoreSet 3A filtering.

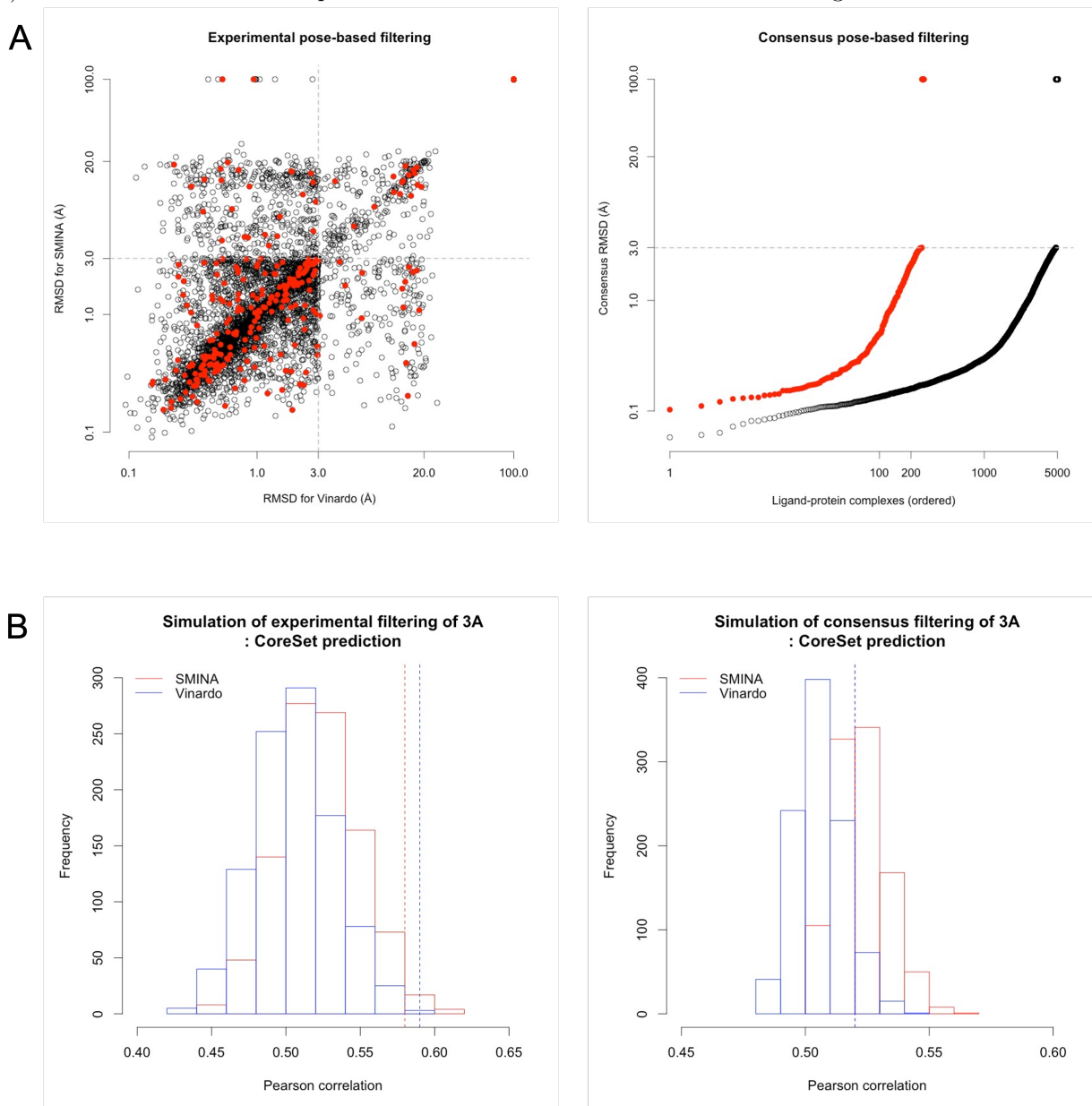
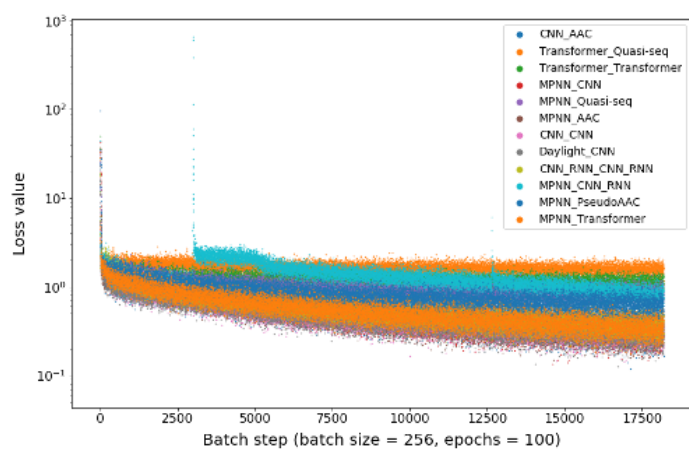


Figure S3. Training and validation of 12 initial BindingDB-trained deep learning models.



	MSE	Pearson	P-value	CI
MPNN_Transformer	0.5807	0.8278	0.0	0.8609
MPNN_CNN	0.5826	0.8254	0.0	0.8611
MPNN_AAC	0.5884	0.8247	0.0	0.8591
CNN_CNN	0.5920	0.8238	0.0	0.8594
CNN_AAC	0.5934	0.8220	0.0	0.8546
Daylight_CNN	0.6134	0.8160	0.0	0.8556
CNN_RNN_CNN_RNN	0.6630	0.8023	0.0	0.8476
MPNN_PseudoAAC	0.7867	0.7575	0.0	0.8161
MPNN_CNN_RNN	0.8167	0.7446	0.0	0.8145
MPNN_Quasi-seq	1.0326	0.8617	0.0	0.7769
Transformer_Transformer	1.1874	0.5921	0.0	0.7278
Transformer_Quasi-seq	1.6344	0.3317	0.0	0.6169

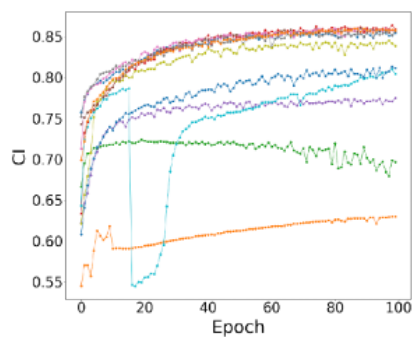
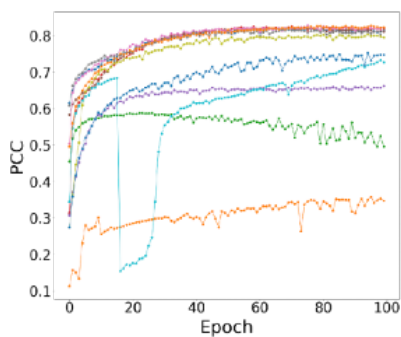
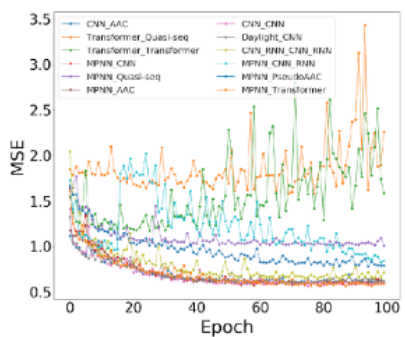


Figure S4. Regression results of the BindingDB Kd data for 66,444 ligand-protein complexes by the BindingDB-trained, PDBbind-trained, and PDBbind-finetuned models.

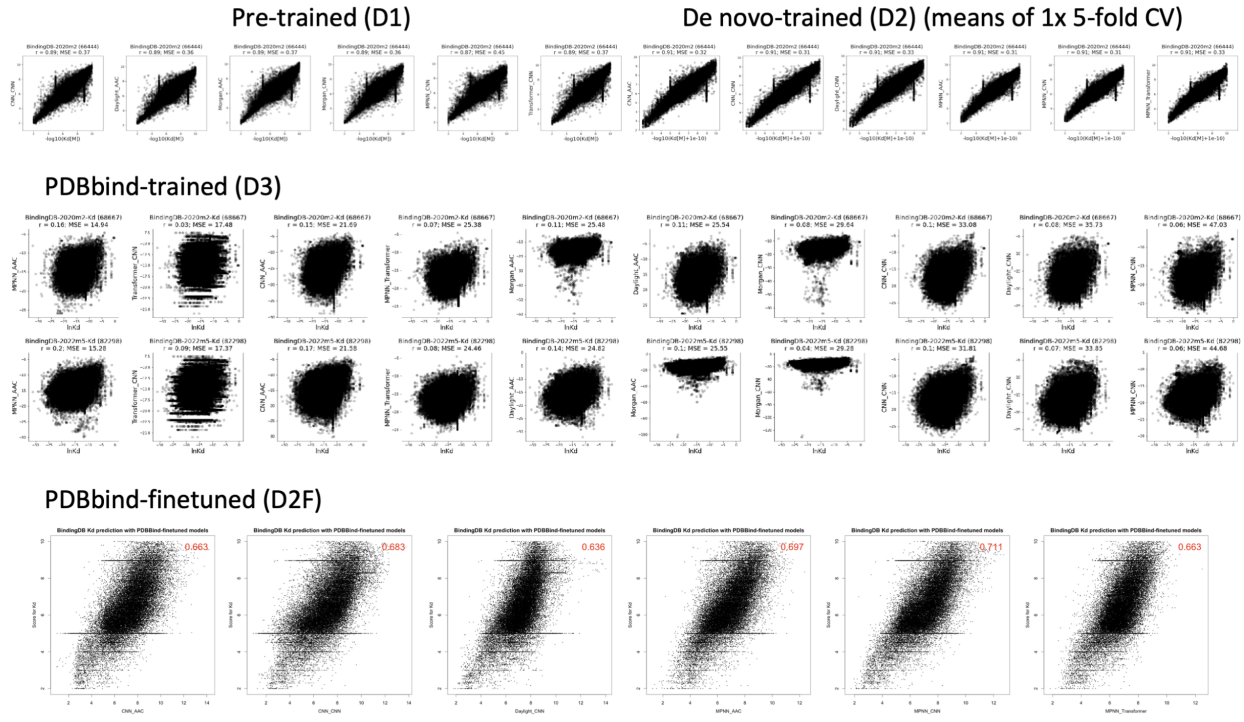


Figure S5. Regression results of the PDBBind-v2020-RefinedSet by the BindingDB pre-trained, BindingDB *de novo*-trained, PDBbind *de novo*-trained, and PDBbind-finetuned models.

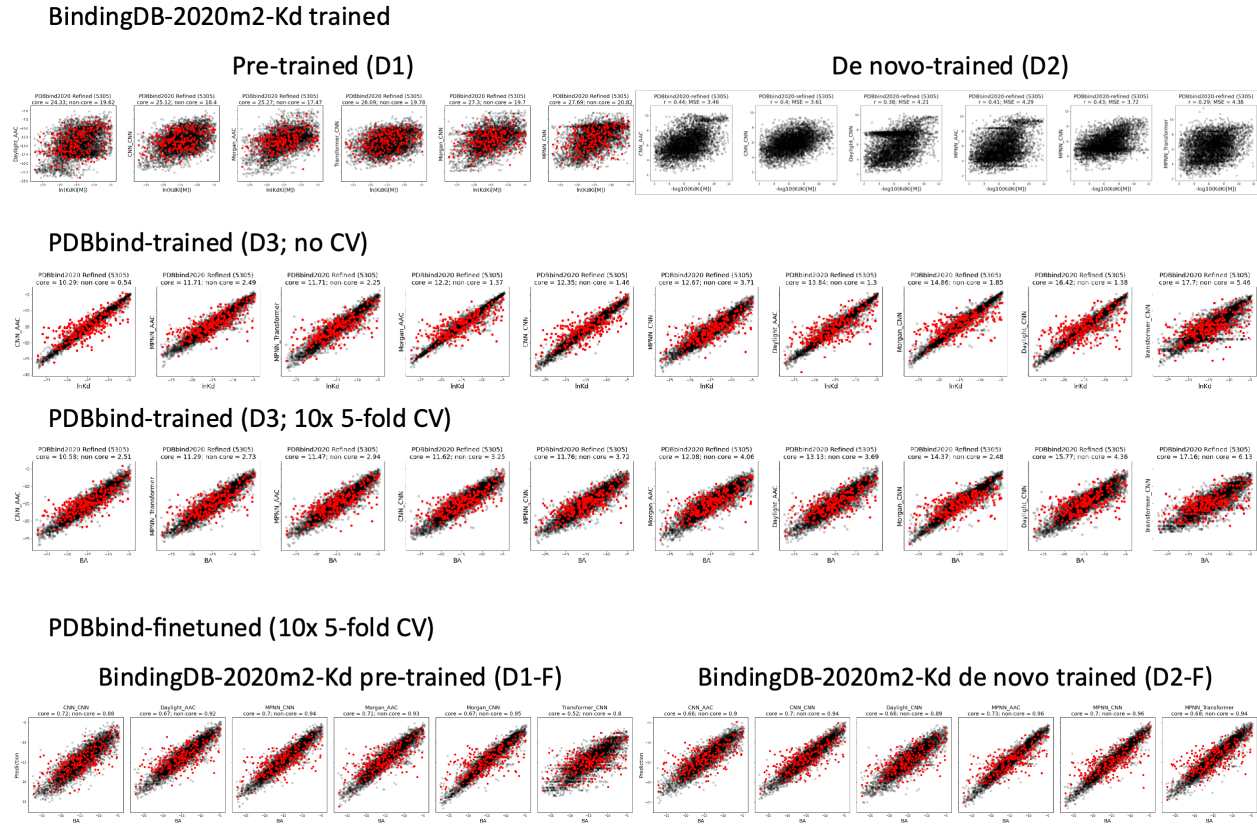


Figure S6. Model comparison of non-core (training set) predictions.

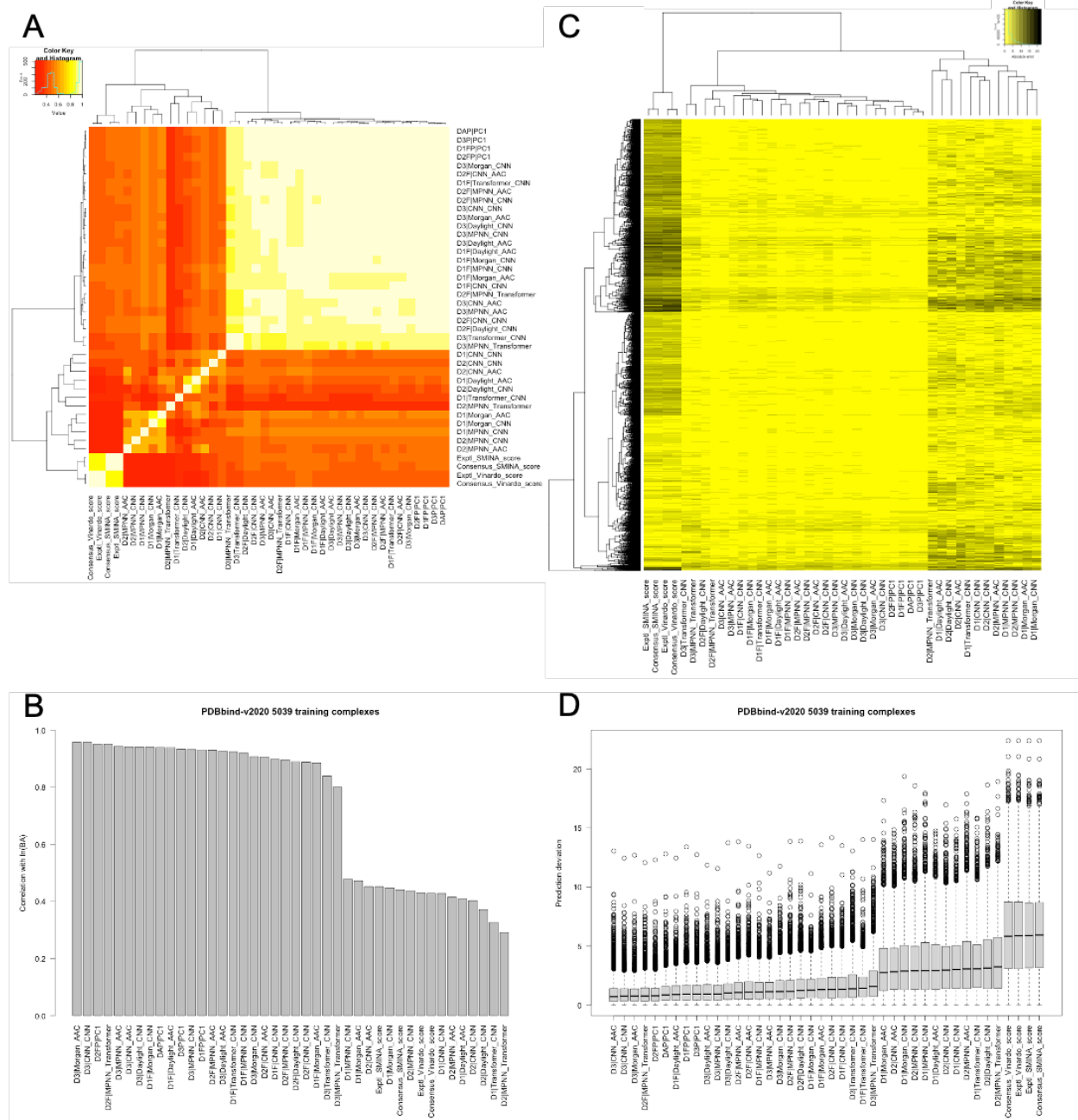


Figure S7. Feature importance of meta-models.

